Layout Optimization of Offshore Wind Farms affected by Wake effects, Cable topology and Support Structure variation

Alvertos Maselis

Master of Science Thesis

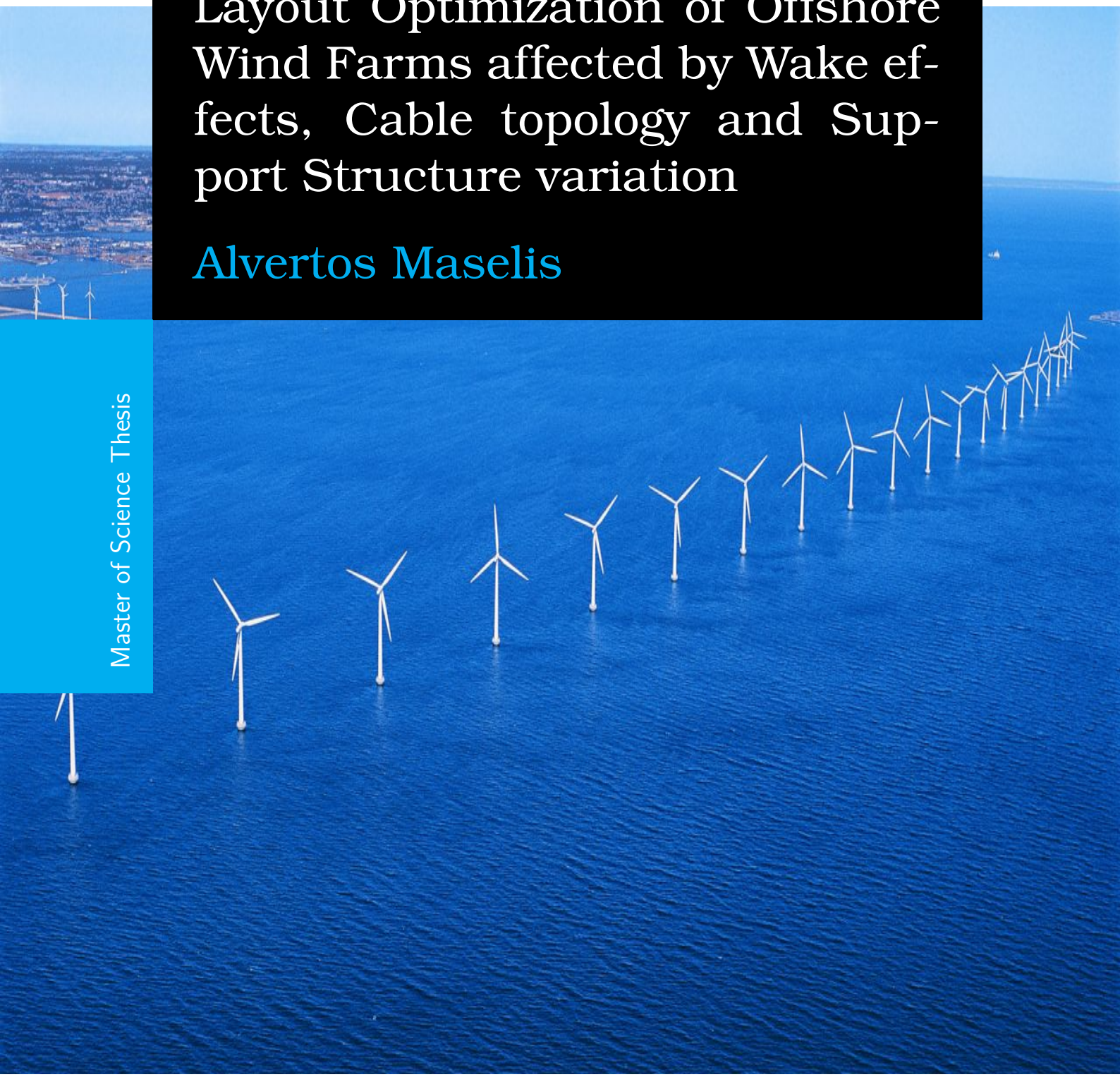

TU Delft Delft University of Technology

Faculty of Electrical Engineering, Mathematics and Computer Science

Layout Optimization of Offshore Wind Farms affected by Wake effects, Cable topology and Support Structure variation

Master of Science Thesis

For the degree of Master of Science in Sustainable Energy Technology
at Delft University of Technology

Alvertos Maselis

October 9, 2016

Faculty of Electrical Engineering, Mathematics and Computer Science

TU Delft Delft University of Technology

Delft University of Technology
Department of
Wind Energy

The following members of the Thesis committee certify that they have read and recommend to the Faculty of Electrical Engineering, Mathematics and Computer Science for acceptance a thesis entitled

Layout Optimization of Offshore Wind Farms affected by Wake effects, Cable topology and Support Structure variation

by

Alvertos Maselis

in partial fulfillment of the requirements for the degree of

Master of Science Sustainable Energy Technology

Dated: October 9, 2016

Supervisor: Dr. ir. Michiel Zaaijer

Thesis committee: Prof. dr Gerard van Bussel

Dr. ir. Michiel Zaaijer

Dr ir. Mark Voskuijl

Abstract

As part of the effort to reduce the cost of offshore wind energy, this MSc Thesis deals with the layout optimization of an Offshore Wind Farm affected by wake effects, cable topology and support structure variation. The main objective of the current MSc Thesis is to investigate how important each of these aspects for the layout optimization is. The final outcome of the project is an optimization tool that tries to find the optimal Offshore Wind Farm (OWF) layout in terms of the lowest Levelized Production Cost (LPC).

This optimization tool depends on the analyzer algorithm, which calculates the objective function of the optimizer. The analyzer consists of three different elements that are combined together so that the Levelized Production Cost will be calculated. Thus, the objective function will be the LPC. The analyzer elements are the wake effects, cable topology and support structure variation.

For the support structure variation, part of the MZ Tool[1] developed by professor Dr. Michiel Zaaijer is used. Using this tool the support structure dimensions and costs can be determined. Regarding the cable topology, a hybrid approach[2] between Planar Open Savings (POS)citekatsouris and Esau-Williams (EW)[2] heuristics is used so that the performance of EW can be improved for multiple cables and lower infield cable cost will be achieved. Finally, the Jensen wake model is used in an algorithm so that the wake effects can be determined. The output of that algorithm is the annual energy yield and the LPC.

The optimization tool is based on the Genetic Algorithm (GA)logic. The performance of the optimization tool is evaluated both cost and time-wise by implementing four scenarios. In these scenarios some parameters of the GA are changed so that the behavior of the optimization tool can be examined.

Finally, different case studies, related to the seabed shape and to the three ingredients in the analyzer, are examined. These case studies will show how the changes in the analyzer can affect the optimality of an OWF. More specifically, it is found that all three elements in the analyzer affect the layout optimization. In addition, it is concluded that the support structure variation has the largest contribution to the layout optimization compared to the cable topology. Regarding the computation time, it is higher in the case that there is support structure variation, since it takes more time for the analyzer to calculate all the costs.

"I've learned in my life that it's important to be able to step outside your comfort zone and be challenged with something you're not familiar or accustomed to. That challenge will allow you to see what you can do."

— *J.R.Martinez* —

Acknowledgements

Foremost, I would like to express my sincere gratitude to my supervisor Michiel Zaaijer for the continuous support of my MSc thesis study and research, for his patience, motivation, enthusiasm, and immense knowledge. His guidance helped me in all the time of research and writing of this thesis.

Moreover, I want to thank the PhD candidate Sebastian Sanchez Perez-Moreno for his help during my MSc thesis and for his will to share his great knowledge and thoughts with me.

In addition, I would like to thank my family and my two sisters, Vasia and Anna for supporting me spiritually and encouraging me throughout my whole studies and my life in general. My friends, both in Delft and Greece, and especially Manos Lyrakis, Makis Gravanis and Christos Tsiourakis deserve also my wholehearted thanks for supporting me in difficult times.

Last but not least, I would like to thank from the bottom of my heart my parents for their love, their support and encouragement throughout my life. Thank you both for giving me the means to succeed my goals and chase my dreams. My MSc thesis is dedicated to my parents.

Delft, University of Technology — Alvertos Maselis
October 9, 2016

Table of Contents

List of Figures

List of Tables

List of Symbols

Latin symbols

A	constant parameter (=0.5)
A_p	cost constant
B_p	cost constant
$C_{capital}$	capital costs excluding management costs
$C_{decommissioning}$	decommissioning costs excluding management costs
$C_{disposal}$	disposal costs
$C_{electrical}$	electrical system costs
$C_{foundation\ installation}$	costs of foundation installation
$C_{O\&M}$	costs of operation and maintenance
$C_{offshore\ works}$	costs of offshore works of rotor-nacelle assembly installation
C_{other}	other costs
C_p	cost constant
C_{RNA}	costs of rotor-nacelle assembly
$C_{removal}$	removal costs
$C_{sup.str.}$	support structure costs
C_t	thrust coefficient
$C_{turbine}$	turbine costs
$Cost_{AC}$	cost of the AC cables
$cos\phi$	power factor
D	diameter
D_W	wake diameter
d	distance between two wind turbines
d_{water}	water depth
E_y	annual energy yield
$f_{warranty}$	warranty percentage of rotor-nacelle assembly costs
h_{hub}	hub height
I	turbulence intensity

I_{rated}	rated current of the cable
k	decay factor
k	shape factor
L	transportation distance onshore
l	length of transmission cable
m_{copper}	mass of copper in cable
m_{grout}	mass of grout
$m_{insulation}$	mass of insulation material in cable
m_{jacket}	mass of jacket of transform platform
m_{pile}	mass of monopile
m_{RNA}	mass of rotor nacelle assembly
m_{tower}	mass of tower
$m_{transition\ piece}$	mass of transition piece
N_t	number of turbines in farm
$P_{farm,rated}$	power rating of wind farm
$P_{shunt,offshore}$	power rating of offshore shunt reactor
$P_{shunt,onshore}$	power rating of onshore shunt reactor
$P_{turbine,rated}$	power rating of turbine
r	real interest rate per period
$r_{offshore}$	winding ratio of offshore transformer
$r_{onshore}$	winding ratio of onshore transformer
S_n	rated power of the cable
$stepx$	x axis - step between possible wind turbine positions
$stepy$	y axis - step between possible wind turbine positions
T	operational lifetime
U	mean wind speed
$U_{free\ stream}$	non-obstructed mean wind speed
U_{rated}	rated voltage of the cable
U_{wake}	wake wind speed
$V_{scour\ protection}$	volume of scour protection
v	inflation rate
x	distance downwind from the rotor
x	horizontal coordinate of a point in farm
x_{max}	maximum x coordinate
x_{min}	minimum x coordinate
x_n	x axis - number of possible wind turbine positions in grid
y	vertical coordinate of a point in farm
y_{max}	maximum y coordinate
y_{min}	minimum y coordinate
y_n	y axis - number of possible wind turbine positions in grid
z	water depth of a specific point in farm

z_0	roughness length

Greek symbols

α	annuity factor
α	scale factor
ΔU	cumulative total deficit
δ	size of the wind speed bins
σ_U	wind speed standard deviation

Chapter 1

Introduction

This Chapter presents background information for wind turbines. In addition, the motivation of the current MSc. Thesis is stated. In the motivation paragraph the importance of the layout optimization of an Offshore Wind Farms (OWF) is mentioned. Subsequently, the objective of the project is mentioned as well as the layout of the report.

1-1 Background information

1-1-1 Offshore Wind Turbines

Installation of wind power offshore is more acceptable to local communities than land installations because noise and visual disturbance is limited. In addition, in case of an OWF, larger arrays of wind turbines on high towers can be installed. Offshore wind turbines have larger power outputs, since they are operating at higher levels above the surface. Another difference between offshore and onshore wind turbines is the fact that in the first case wind speed is higher, while turbulence intensity is lower. The majority of OWF are built in shallow waters, close to shore, and as a result flow conditions are affected by land. The larger the distance from the shore, the higher the wind speed and the lower the turbulence intensity.

1-1-2 Wind turbine power output variation

Wind turbines start operating as the mean wind speed exceeds the cut-in wind speed, which values are between $3 - 5\ ms^{-1}$ depending on the type of the wind turbine. The power output rises when the wind speed increases above the cut-in speed. The electrical power output reaches the limit that the electrical generator is capable of, somewhere between 12 and 17 meters per second. For higher wind speeds the power production is steady regardless of the wind speed up to cut-out wind speed of 25 ms^{-1}. At the cut-out wind speed, wind turbines are shut down for safety reasons.

Figure 1-1 illustrates the wind turbine power output variation with steady wind speed.

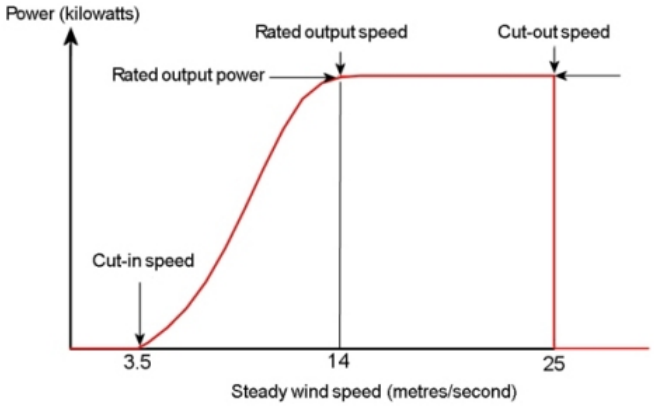

Figure 1-1: Wind turbine power output variation with steady wind speed [3].

1-2 Problem Analysis

Nowadays, conventional fossil fuels are running out due to high and continuous energy demand and they are going to become too expensive in the near future. A future that relies on renewable energy will guarantee the future of the upcoming generations. For these reasons, sustainable energy technologies have been emerged in the past decades. These energy sources are inexhaustible and their use causes no pollution to the environment. There are many types of Renewable Energy Sources (RES) such as wind energy, solar energy, biomass, hydroelectric and geothermal.

Wind energy and especially offshore wind energy is a very promising technology, since it is still the fastest growing source of energy in the world today. Over the past decades OWF have gained attention and more and more wind parks are built. Stronger wind speeds are available offshore compared to on land and as a result offshore wind power's contribution in terms of electricity supplied is higher and NIMBY (Not in my back yard) opposition to construction is usually much weaker.

However, offshore wind farms are relatively expensive. Offshore wind energy has high Levelized Cost of Electricity (LCOE) compared to fossil fuels and other renewable sources. This occurs due to high investment and operation and maintenance costs. More specifically, wind turbines, electrical infrastructure, support structure, installation and maintenance contribute all to the LCOE in the case of an OWF. Furthermore, currently the cost of energy of offshore wind energy is still greater than that of on shore. However, the cost of energy of offshore wind farms can be decreased through a reduction in the cost or through an increase in the energy production.

The layout of an offshore wind farm is one potential means of reducing the cost of energy. The turbines in most of the large, existing offshore wind farms (e.g. Horns Rev, Nysted, North Hoyle, Kentish Flats, Barrow-in-Furness, and Egmond aan Zee) are organized in rectilinear grids. This approach, while simple to implement, may miss an opportunity to increase the wind farm energy production or lower the wind farm cost.

Apart from the way that the wind turbines are organized inside the farm, there are also some other parameters that affect the optimality of the OWF layout. These parameters are the

wake effects, the cable topology and the support structure variation.

The wakes effects are dependent on the distance between the wind turbines. The closer the wind turbines are, the larger the wake losses are. So, this has a negative impact to the total energy output of the farm and to the cost of energy.

The cable topology affects also the optimality of the layout, because the costs increase when the cable length is larger. Larger cable length means larger distance between the turbines.

Finally, the support structures play an important role to the final OWF layout. The support structures need to be designed specifically for each site, due to wide design parameters variation; even within the wind farm some conditions might differ. So, for different water depths inside the farm, different support structure designs may be needed. The deeper the water depth is, the more expensive the support structure will be. In addition, wave height is another parameter of great importance since it also affects the design of the support structure by exerting forces and moments on the structure. Furthermore, the load caused by waves crashing against the substructure very close to the foundation depends on the wave height. Taking all the above into consideration, support structure plays an important role in the overall concept design for offshore wind farms and as a consequence to the final cost of the OWF.

1-3 Objective

The main objective of the Master Thesis is to determine the importance of each of the following three ingredients for the layout optimization.

In order to achieve the main objective, some sub-goals should be also achieved. Thus, it is important to examine how to capture the effect of these ingredients on optimality, how to implement these ingredients and how to realize the optimization by simultaneously considering these three ingredients.

The aforementioned ingredients are mentioned as follows:

- Wake effects,
- Cable topology and
- Support structure variation.

Specifically, the current work consists of two parts, the analyzer and the optimizer. The analyzer is an algorithm, which combines the wake effects, the cable topology and the support structures of the wind turbines. The second part is the optimization tool, which will try to find the best layout of the offshore wind farm in terms of the lowest Levelized Production Cost (LPC). Îđhe LPC will be the objective function and the developed optimization tool will try to minimize the LPC. There several ways to calculate LPC and this will be defined later on, in the following chapters. The layout of an OWF can be optimized if the LPC can be determined based on the turbine positions, which constitute the most important design consideration.

1-4 Approach

As it has already been mentioned in section 1-3, the first part of the current work will be the analyzer and the second one will be the optimizer.

Both parts have some common inputs such as the layout of the wind turbines, the site conditions, the wind turbine characteristics, the electrical system data, the wind rose, the shape of the seabed and the LPC parameters.

Almost all of these inputs are used by the analyzer. Each one of the 3 ingredients inside the analyzer plays an important role in finding the most optimal positions of the wind turbines, as it has been mentioned in subsection 1-2. The modelling of these 3 ingredients will be treated in later chapters. It must be also noted that the algorithm used for the wakes is developed by the PhD candidate Sebastian Sanchez Perez Moreno[4]. For the cable topology Georgios Katsouris algorithm[2] is used and for the support structures the MZ tool [1], developed by Dr. Michiel Zaaijer, is implemented.

The final outcome of the analyzer is the Levelized Production Cost, which is the objective function of the optimizer. That means that the optimizer tries to find the layout with the lowest LPC value, which is calculated through the analyzer. So, the output of the optimizer is a new wind farm layout with a specific number of wind turbines. Both the new layout and the number of turbines are used as inputs by the analyzer and a new LPC is calculated.

The optimizer is generated as many times as the lowest LPC is achieved. A more detailed description of the optimizer is given in chapter 7.

From the above process several results can be extracted:

- The final layout of the wind farm,
- The value of the lowest LPC,
- The annual energy yield of the farm,
- The support structure cost for each wind turbine and
- The cable layout.

Figure 1-2 illustrates a general overview of the process that will be followed in the following chapters.

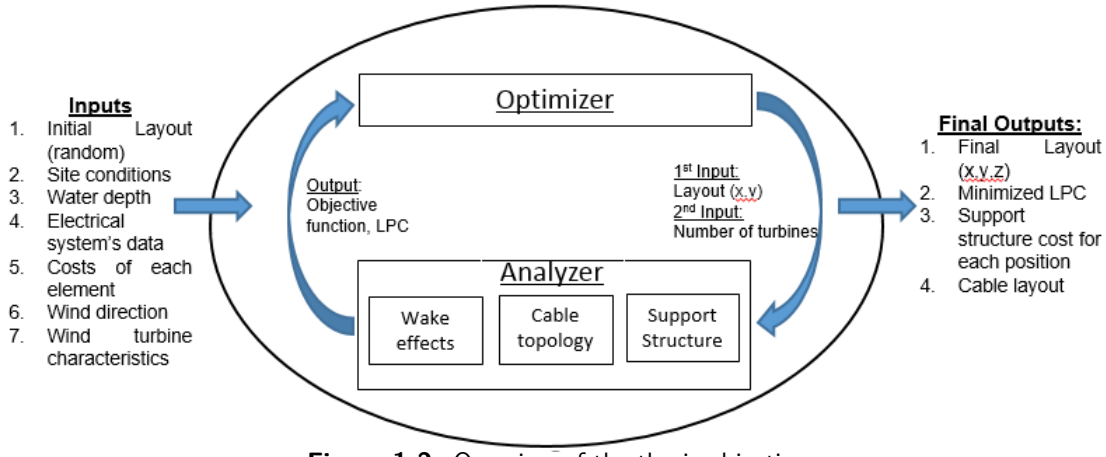

Figure 1-2: Overview of the thesis objective.

In addition, it must be noted that for both the analyzer and the optimization algorithm, Python software [5] was implemented.

1-5 Layout of the Report

The layout of the report is organized as follows:

Chapter 2 provides the way of calculation of the Levelized Production Cost that is going to be the objective function for the current MSc Thesis. In this chapter the effect of the 3 ingredients on optimality is investigated.

Chapter 3 presents an overview of the wake effects and describes the wake model used in the current work. In addition, the way of wake calculation for the current work is provided.

Chapter 4 is referring to the electrical system. An overview of the electrical collection system designs for OWF and a comparison between single and multiple cables is given. Furthermore, a description of the algorithm used for the infield cost cable is presented.

Chapter 5 treats the Offshore Wind Farm support structures.

Chapter 6 gives an overview of the analyzer. Results from the analyzer are also provided. Moreover, the analyzer use Horns Rev wind farm as a case study.

Chapter 7 provides a description of the optimization tool used in the thesis. Moreover, different case studies are being developed for the performance of the optimizer. So, in this chapter it is investigated how to realize the optimization by simultaneously considering the 3 different ingredients.

Chapter 8 treats the results derived from the implementation of the optimization tool.

Chapter 9 presents the conclusions and recommendations of the thesis.

Chapter 2

Levelized Production Cost (LPC)

This chapter gives an overview of the Levelized Production Cost, LPC. More specifically, this chapter provides the way of LPC calculation and the calculation of all the parameters that are involved in the LPC equation.

2-1 LPC calculation

The LPC is going to be the objective function for the purposes of the current work, as previously mentioned in section 1-3. The objective function is used for the optimization algorithm, since as its name suggests, it is the main target that the optimization algorithm strives to maximize or minimize. For the current case the algorithm is going to minimize the objective function and as a consequence to minimize the levelized production cost.

The cost of energy can be defined in different ways but the simplest approach is to take the ratio between total costs and the energy yield. The LPC is given by the following formula, Equation 2-1:

$$LPC = \frac{C_{Inv}}{\alpha * E_y} + \frac{C_{O\&M}}{E_y} + \frac{C_{Decom} * (1+r)^{-T}}{\alpha * E_y} \tag{2-1}$$

where:

- C_{Inv} is the investment costs,
- $C_{O\&M}$ is the operation and maintenance costs,
- C_{Decom} is the decommissioning costs,
- α is the annuity factor,
- T is the operational lifetime,

- r is the real interest rate per period and
- E_y is the annual energy yield.

The annuity factor is given by Equation 2-2:

$$\alpha = \frac{1.0 - (\frac{1.0}{1.0+r})^T}{r} \tag{2-2}$$

and the real interest rate is calculated by Equation 2-3:

$$r = \frac{1.0 + i}{1.0 + v} - 1.0 \tag{2-3}$$

where i is the interest rate and v is the inflation rate. The aforementioned values are assumed to be 0.1 and 0.025 respectively.

In addition, the operational lifetime is assumed to be 20 years, since almost all the modern wind turbines are designed to work 20 years.

The investment, operation and maintenance costs and the decommissioning costs are going to be analyzed in the following subsections 2-2-1,2-2-2 and 2-2-3.

Finally, the annual energy yield is described in section 2-3.

2-2 Cost Components

2-2-1 Investment costs

The investment costs for an offshore wind farm can be given by Equation 2-4.

$$C_{inv} = C_{turbine} + C_{sup.str.} + C_{electrical} + C_{installation} + C_{other} \tag{2-4}$$

where $C_{turbine}$ are the turbine costs, $C_{sup.str.}$ are the costs for the support structure of the wind turbine, $C_{electrical}$ are the costs of the whole electrical system, $C_{installation}$ are all the installation costs for the foundations, rotor−nacelle assembly, auxiliary and electrical system.

Although some of the cost components above are fixed, some of them are affected by the 3 ingredients in the analyzer.

More specifically, the support structure costs are not fixed, since in the current work each wind turbine uses a different support structure design according to the water depth. Thus, the cost for each support structure will be different.

In addition, the infield cable cost is calculated by using the algorithm in [2] where the cable cost is not fixed, but affected by the layout of the wind farm. Apart from the infield cable cost, all the other cost components of the electrical system use a fixed cost value. These cost components are the transmission cable, the shunt reactor and the transformer.

Regarding the installation costs, the installation cost of the infield cable is variable since the length of this cable(calculated by [2] is not fixed, see Equation 2-5. Furthermore, the installation costs both for foundations and for onshore transport are not fixed, since they depend on the mass pile and diameter respectively, see Equations 2-6 and 2-7. All the other installation cost components have fixed cost values. These cost components are the offshore works, the transmission cable, the dune crossing, the meteo tower and the harbor use.

$$C_{infield\ cable\ installation} = 500,000 + 169 * l \tag{2-5}$$

where 500,000 is the fixed cost for cable laying in Euros and 169 is the cost for cable laying per distance in Dollars. For the currency conversion see subsection 2-2-4.

$$C_{foundations} = 1.4 * m_{pile} * N_t \tag{2-6}$$

where 1.4 is the cost for the foundation installation per meter and it is expressed in Dollars, see subsection 2-2-4.

$$C_{onshore\ transport} = (5.84 * 10^{-3} * D + 0.4) * L + 0.486 * D^{2.64} \tag{2-7}$$

where 5.84, 0.4, 0.486 and 2.64 are coefficients used for the onshore transport.

Finally, the investment costs related to the rotor-nacelle costs such as purchase and warranty are also fixed. They depend only on the number of the wind turbines and they are not affected by any variable parameter.

Furthermore, a percentage of 0.03 of the total investment costs was used in order for the management costs to be included as well.

For a more detailed description of the mathematical formulas of the cost models is given in subsection 2-2-4.

2-2-2 Operation and Maintenance costs

The O&M costs are completely independent on the layout, but the site conditions have a great influence on these costs. Both the fixed and variable operation and maintenance costs consist a very important part of the total LPC.

However, no complete mathematical models for these costs were found in the literature. In the current Thesis a very simplified model will be implemented. Thus, a simple model of the annual O&M costs is a fixed percentage of the investment costs. Based on [6] the annual O&M costs are approximately equal to 6% of the total investment costs.

In addition, it must be noted that the analyzer uses the aforementioned model for the calculation of the O&M costs. However, the optimizer uses this cost model only for the LPC calculation of the initial population, see section 7-1. Subsequently, the average O&M value is calculated and it is used as fixed value for all generations, see section 7-1.

2-2-3 Decommissioning costs

The decommissioning costs for an offshore wind farm can be given by the following Equation 2-8.

$$C_{decom} = C_{removal} + C_{disposal} \tag{2-8}$$

The $C_{removal}$ component includes several costs such as rotor-nacelle assemblies, foundations, infield cable, transmission cable, offshore platform and meteo tower, scour protection and site clearance costs. The second component of Equation 2-8 includes the rotor-nacelle assemblies costs. From all these costs only the removal cost of the infield cable is not fixed since it depends on the infield cable length.

The management of the decommissioning costs is also required and it represents 0.03 of the total decommissioning costs.

2-2-4 Mathematical formulas of cost models

All the mathematical descriptions that were used for the calculation of both the investment costs and decommissioning costs were taken by [1]. In Appendix B the formulas for the aforementioned calculations are provided. The values of some parameters used in these formulas are also taken by [1]. These parameters are the $f_{warrnty}$, m_{copper}, $m_{insulation}$, $r_{turbine}$, $r_{onshore}$, $r_{offshore}$, $P_{shunt,offshore}$, $P_{shunt,onshore}$ and the transmission cable length l. Other parameters such as m_{pile}, m_{tower}, $m_{transition\ piece}$, m_{grout}, $V_{scour\ protection}$ are not fixed and they are calculated inside the code.

At this point it is of great importance to mention that many of the mathematical descriptions for all the aforementioned costs are not expressed in Euros. Thus, a function was created in order to convert different currencies into Euro currency. For that purpose the inflation rates and the exchange rates to Euro were used. This information is provided in Table B-1.

Table 2-1: Applied inflation rates and exchange rates to Euro

Currency	Annual inflation rate (%), averaged over 2000-2015	Exchange rate
USD	2.57	0.89
GBP	2.55	1.27
DKK	1.84	0.13
SEK	2.03	0.11
NOK	1.95	0.11
Euro	2.16	1.0

2-3 Energy Yield

For the calculation of the annual energy yield of the Offshore Wind Farms (OWF), a series of specific steps must be followed.

At first, the extracted power, including wake effect, from the offshore wind farm must be calculated. For that calculation the code of the PhD candidate Sebastian Sanchez Perez Moreno was used [4], who used Jensen model. Due to the fact that a wind rose was also implemented allowing multiple wind directions, the calculation of partial wake incidence also examined. The wind rose uses as many cardinal directions as the user wants to examine, see subsection 3-4-1. Thus, the delivered power is found for each wind direction and each wind speed.

In addition, it is known that the wind is not steady and in order to calculate the power delivered by a wind turbine from its power curve, it is necessary to know the probability density distribution of the wind speed. Thus, Weibull wind speed distribution have to be included, see section 2-4.

By having both the wind speed and wind direction probabilities, then the total amount of hours, corresponding to a specific wind speed and wind direction, can be calculated. This process can be described by the following equation:

$$hours = 8760 * P(U, \phi) \tag{2-9}$$

where the number 8760 corresponds to the total hours during one year and $P(U, \phi)$ is the probability of a specific wind speed in a specific wind direction.

Lastly, the annual energy yield can be found by the summation of the products of the hours with the corresponding delivered power, Equation 2-10.

$$AEP = hours * \sum_{1}^{Nt} P_{turbine} \tag{2-10}$$

where $P_{turbine}$ is the power delivered by a wind turbine and N_t is the total number of wind turbines.

2-4 Weibull Distribution

In the current work cumulative Weibull wind speed distribution is used. The equation of hte cumulative Weibull distribution is given below:

$$Weibull = 1 - \exp\Big(- \Big(\frac{U \pm \delta}{\alpha} \Big)^k \Big) \tag{2-11}$$

where U is the wind speed, α is the scale factor, k is the shape factor and δ is the size of the wind speed bins.

Tool allows the user to change easily the size of the wind speed bins. In the current work δ is equal to 0.5, while the scale and shape factors are equal to 10.71 and 2.33 respectively.

Chapter 3

Wake Effects

This chapter gives an overview of the first ingredient of the analyzer, which is the wake effects. In addition, the wake model used in the current work is also presented.

3-1 Introduction

The term "wake effect" originates from the wake behind a ship. In general, ship wakes are three ship-lengths long and include the following two phenomena:

- a turbulent wake, which forms directly behind the ship, and
- a Kelvin wake. This wake is wedge-shaped, which means that it starts from the ship's hull and fans out behind the ship; the Kelvin wake is bisected by the turbulent wake.

A wake is the downstream region of disturbed flow, usually turbulent, caused by a body moving through a fluid. In the case of wind turbines, as the wind approaches the rotor plane of a single wind turbine, then pressure increases and air is deflected around the rotor plane. This fraction of the wind is never used to drive the turbine. Kinetic energy is extracted from the fraction of wind passing through the turbine rotor plane. A maximum of 16/27 (59%) of the kinetic energy of the wind can be converted to power (Betz, 1920). Energy extraction slows down the wind and the wind speed measured just downstream of a turbine is significantly lower than the free stream velocity. Near hub-height, the air is also more turbulent. The downstream region, over which the wind climate is affected by a wind turbine, is called a wind wake. The wake velocity deficit (VD) is given by the following expression [7]:

$$VD = \frac{U_{freestream} - U_{wake}}{U_{freestream}} * 100\% \tag{3-1}$$

where $U_{freestream}$ is the non-obstructed mean wind speed and it is observed upstream of a wind farm and U_{wake} is observed in the wake.

Both $U_{freestream}$ and U_{wake} are generally derived from meteorological time-series observations at fixed points in space. Apart from the velocity deficit, there is also another parameter by which wind wakes are characterized. This parameter is turbulence intensity, I and it is given by the following formula:

$$I = \frac{\sigma_U}{U} * 100\% \tag{3-2}$$

where

- U is the mean wind speed and
- σ_U is wind speed standard deviation.

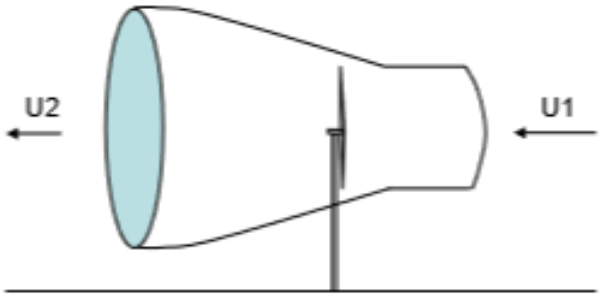

Figure 3-1: Wake downstream of single wind turbine. U_1 and U_2 are upstream and downstream wind speeds, respectively [7].

Assuming that there is no compression, then the amount of air leaving the turbine rotor plane equals the amount entering. Figure 3-1 illustrates how the above principle leads to this wake. The wake radius increases with the downstream distance and when the radius exceeds the turbine hub-height, the wake impacts the surface. This occurs at a downstream distance equivalent 10 rotor diameters [7].

As far as the wake mixing is concerned, there two main reasons that cause wake mixing. These reasons are:

- Wake mixing due to turbulence generated within the shear layer of the wake.
- Wake mixing due to atmospheric turbulence.

These two factors are key determinants of the wake rate of recovery, it means how rapidly the wake is dissipated and the wind flow recovers its initial state. The atmospheric term is dominant in most practical situations and influences at high level the wake velocity field. When describing wind turbine wakes, two sections are normally categorized: the near wake and the far wake. The near wake has been found to be a complex region, comprised within a distance of 2 to 4 rotor diameters downstream from the nacelle. In this region the kinetic energy extraction causes three phenomena to occur:

- A flow pressure drop at the rotor plane.
- A reduction in the centerline velocity
- An expansion in the wake width downstream from the rotor plane.

The last two aspects are shown in Figure 3-2 where the wind speed profiles are drawn in front and behind the turbine. Note that only the upper half is presented, assuming symmetry along the horizontal axis (axisymmetric).

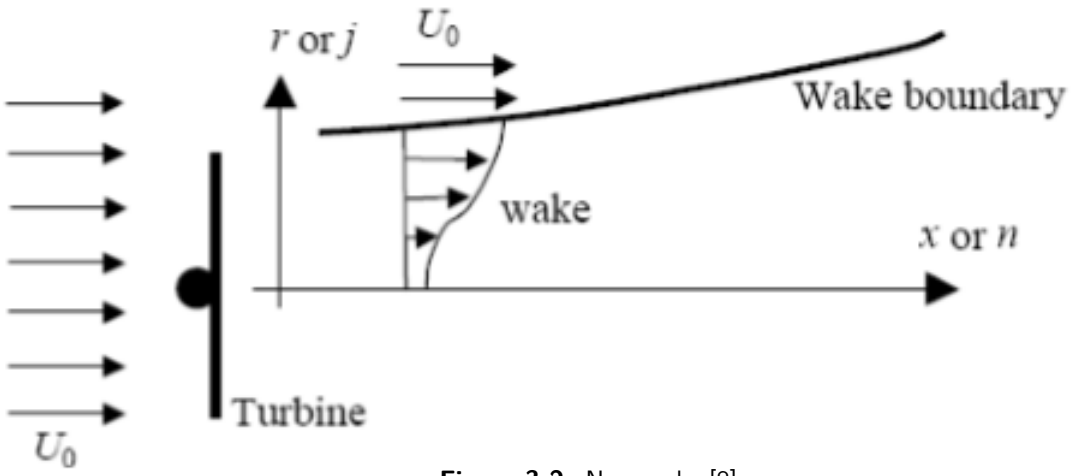

Figure 3-2: Near wake [8].

The minimum centerline velocity happens between 1 and 2 diameters. Beyond this point, turbulent mixing starts to have greater influence over flow characteristics and the velocity profile becomes more similar to the initial undisturbed situation.

3-2 Wake models

3-2-1 Introduction to wake models

Wind turbine wakes are generally divided in the near wake, where the influence of the separate rotor blades can be distinguished, and the far wake. Although the naming may imply otherwise,there is a gradual transition from one to the other, not an abrupt one. Different studies suggest different lengths for the near wake, ranging from one to a maximum of several rotor diameters. In recent years quite some research has been done on modeling the near wake. Typical models describing the near wake are the asymptotic acceleration potential method, vortex wake models and generalized actuator disc models. While some of these methods have been applied to study the flow through several wind turbines, they are computationally too intensive to use for general wind farm calculations. Far wake models can be divided in kinematic wake models (also called explicit models) and field models (or implicit models).

The most known wake models are the Jensen wake model, the Frandsen model and the Ainslie model. For the current MSc Thesis the Jensen wake model described in subsection 3-2-2 is implemented. Thus, for the calculation of the wind speed deficit in a turbine wake, the wake expansion diameter and the total power extracted from the Offshore Wind Farms (OWF) the equations of Jensen wake model will be used.

3-2-2 Jensen model

N.O. Jensen model [9] is one of the oldest wake models, and further developed by I. Katic. This wake model is quite simple and assumes a linearly expanding wake with a velocity deficit that is dependent of the distance behind the rotor and of the decay factor. It is based on the description of a single wake and considers the initial velocity reduction and a wake decay coefficient. In addition, it is assumed that the wind velocity inside the wake does not change.

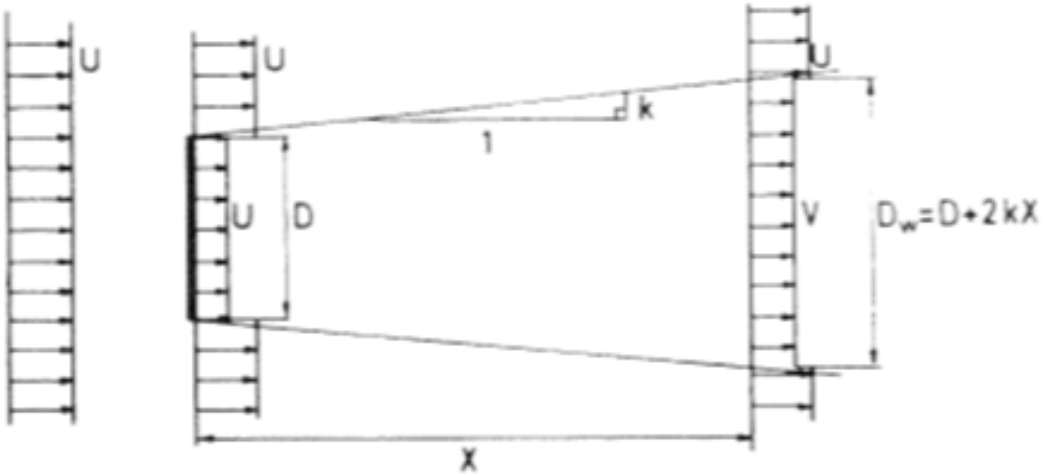

Figure 3-3: Jensen wake model [9].

Figure 3-3 illustrates the wake at a horizontal plane through the rotor of a wind turbine. Initially, the wake diameter is equal to rotor diameter and then, as it has already been mentioned, it spreads in a linear way as a function of distance. Typical spacing between wind turbines is 4 to 10 rotor diameters. For a smaller distance between them, the results of the wake velocity function are not so accurate.

The wake diameter is given by:

$$D_w = D_0 + 2 * k * x \tag{3-3}$$

where k is a constant called the decay factor and it describes the dissipation of the wake by growth of width. The decay factor is affected by several parameters such as wind speed, atmospheric stability, turbine induced turbulence and ambient turbulence. The decay factor is equal to 0.075 and 0.05 for onshore and offshore conditions respectively.

Finally, the decay factor can be calculated by the following formula:

$$k = \frac{A}{ln\frac{h}{z_0}} \tag{3-4}$$

where:

- h is the height
- z_0 is the roughness length
- A is a constant ($\simeq$0.5)

The velocity deficit of the wake at position X is:

$$1 - \frac{V}{U} = \frac{1 - \sqrt{1 - C_t}^2}{1 + \frac{2kX}{D_0}} \tag{3-5}$$

Or

$$\vartheta V = U - V = U(1 - \sqrt{1 - C_t})\Big(\frac{D}{D + 2kX}\Big)^2 \tag{3-6}$$

where C_t is the thrust coefficient of the wind turbine as function of the wind speed and it can be obtained from the manufacturer, from published data or estimated from the turbine power curve.

Thus, from these two equations both the wake width and the speed deficit can be determined.

3-3 Algorithm of Jensen wake model

As it has already been mentioned, the algorithm from [4] was used so that the annual energy yield and the total extracted power of the OWF will be calculated, including the wake effects.

In this algorithm, the wind turbines are ordered by their relative position to the wind front. So, this process will solve the flow conditions at the most upstream wind turbine first and then the second one until the last wind turbine. Furthermore, it calculates exactly both the thrust coefficient and the local wind speeds at all wind turbines inside the farm[4].

In addition, regarding the mixing wakes the following process has been followed. For each wind turbine inside the farm, the wind speed deficits induced by all other N_t turbines in front of it are known. So, the cumulative total deficit ΔU was obtained by taking the square root of the sum of the squares of the individual deficits ΔU. This process is described by the equation below[4]:

$$\Delta U = \sqrt{\sum_{i=0}^{N_t} (\Delta U_i)^2} \tag{3-7}$$

Finally, partial shadowing was also taken into account for the turbines placed along the boundary of a wake. So, the area of the intersection between the rotor and the wake is calculated to determine the weighted average deficit over the whole rotor area[4].

3-4 Parameters

The inputs for the wake model are the coordinates of the wind turbines, the power curve, the thrust curve as well as the decay constant and the turbine rotor diameter . In addition, another parameter of great importance is the wind direction. It is very meaningful, since the outcome differs according to the different wind directions and different wind speeds. Thus, the Jensen wake model is implemented by taking into account all the above parameters in order to be ensured that it covers all the possible cases.

3-4-1 Wind direction and wind speed

Regarding the wind direction, different number of directions was taken into consideration. More specifically, different windrose angles/windrose sectors were examined in terms of accuracy of the results and computation time. A more detailed description of the number of sectors selected is given in subsection 6-2.

As far as the wind speed is concerned, a range from 4 ms^{-1} to 25 ms^{-1} was taken into account. This range is referring to the wind speeds from cut-in speed to cut-out speed. This range of wind speeds was selected, since the turbine first starts to rotate and generate power at cut-in speed and the rotor stands still at cut-out speed. Thus, the turbine operates inside this range of wind speeds.

3-4-2 Power and Thrust curves

Both power and thrust curves are specified by turbine manufacturers and they are different for different types of wind turbines. In the current work the user has the possibility to change these two curves according to the type of wind turbine that he/she wants to use.

3-4-3 Decay constant

As far as the decay constant is concerned, it describes the dissipation of the wake by growth of its width, see subsection 3-2-2. For the offshore conditions the value of decay constant is equal to 0.05.

Lastly, the turbine rotor diameter is also an important parameter for the calculations of the Jensen wake model and it depends on the type of the implemented wind turbines.

Chapter 4

Electrical Collection System for Offshore Wind Farms (OWF)

This chapter gives an overview of the electrical system of OWF. More specifically, it describes the collection system, the different designs of the electrical collection system and the radial and branched Offshore Wind Farm Infield Cable Topology Problem (OWFICTP).

4-1 Electrical Collection System for OWF Overview

The electrical system for an Offshore Wind Farm (OWF) consists of six key elements:

- Wind turbine generators,
- Offshore inter-turbine cables (electrical collection system),
- Offshore substation,
- Transmission cables to shore,
- Onshore substation (and onshore cables) and
- Connection to the grid.

A typical electrical single line diagram of an offshore wind farm is illustrated in Figure 4-1.

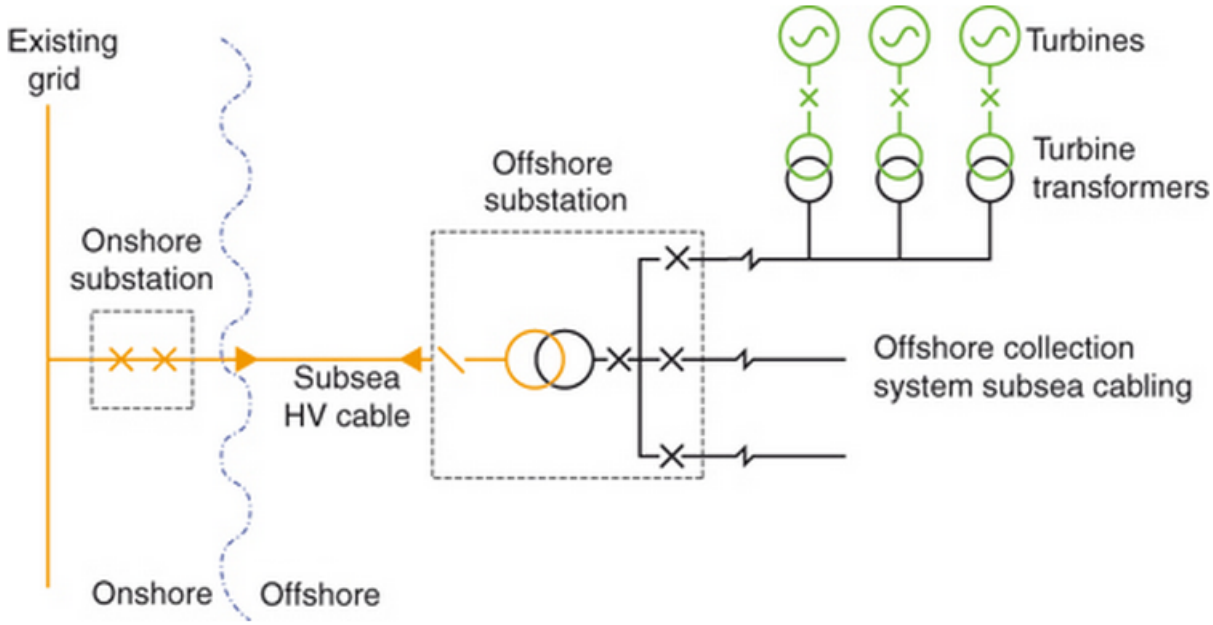

Figure 4-1: Typical single line diagram [10].

The design of the electrical system is determined by the characteristics of the wind turbine generators and of the network to which the wind farm is to be connected, as well as regulations that are referred in Grid Codes[9].

4-2 Electrical Collection System Designs

There are mainly four different possible connection designs. The decision about which of these designs is going to be used in an offshore wind farm depends on two reasons. The first one is the size of the OWF and the second one the desired level of reliability. In past years, the majority of the OWF were small and as result much more simple collection designs were used and reliability was not the primary factor. However, nowadays offshore wind farms are getting larger and larger and reliability must be taken into account, since the amount of energy lost during a fault might be high enough to overcome the initial costs of a design that provides reliability to the wind farm.

The aforementioned electrical collection system designs are known as radial, ring, star and branched. In the following subsections, an overview of these designs follows.

4-2-1 Radial Design

In the radial collection system, the wind turbines included within the same feeder are installed in a string configuration, Figure 4-2.

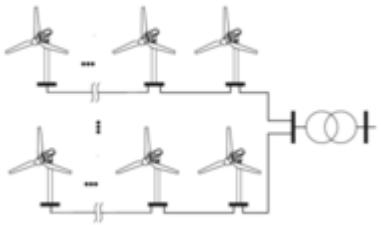

Figure 4-2: Radial collection configuration [11].

The maximum number of wind turbines that can be connected to one feeder is determined by the cable capacity and the rated power of the generators. This design is cheap, common and simplest collection system, but its drawback is the low reliability. This is due to the fact that if a failure occurs in the cable connecting the first turbine and the hub of the feeder, all the power generated by the downstream wind turbines in the string will be lost [11].

4-2-2 Ring Design

The second electrical collection system design is the ring design [11]. Ring design has high reliability, but it is much more expensive in comparison with the radial one. Depending on how the ring is formed, the ring design is divided in three different categories:

- Single-sided ring (Figure 4-3),
- Double-sided ring (Figure 4-3) and
- Multi-ring.

In all cases, redundant cables are added so that the power flow within a feeder have more options to be transmitted. Thus, in the first case, single-sided ring, a cable from the outermost turbine in the feeder is connected to the collector hub. As far as the double-sided ring case is concerned, two feeders are connected together by means of a cable. The drawback is that some cables must be oversized to allow bidirectional power in case of a cable failure.

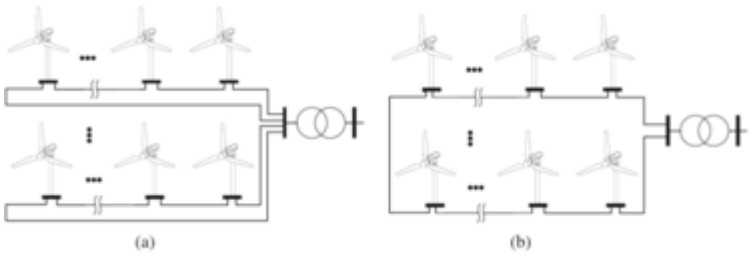

Figure 4-3: Ring collection configuration. (a) Single-sided ring example. (b) Double-sided or multi-ring examples. [11].

4-2-3 Star Design

The star collection system [11] aims to reduce the cable ratings of the cables which connect the wind turbines and the collector point. Such common point is usually located in the middle of all wind turbines disposition, see Figure 4-4.

The advantage of this topology is that the reliability of the system increases, since a cable failure causes the loss of only one machine. On the other hand, due to the longer cable lengths and the use of lower voltage ratings for the connection of wind turbines in this system type, cable losses and their costs are significantly higher than in the aforementioned designs.

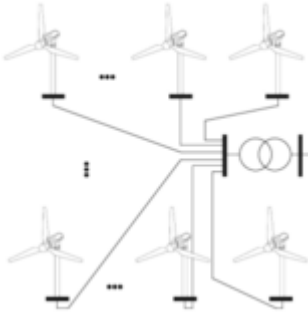

Figure 4-4: Star collection configuration. [11].

4-2-4 Branched Design

The fourth design is known as the branched design [2], see Figure 4-5. In this design there are more than one endpoints that are created by adding branches to the main feeder. Nowadays, branched topology is used more and more often in OWF.

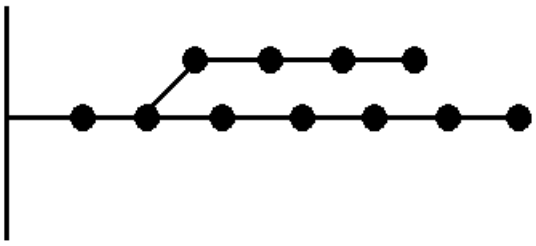

Figure 4-5: Branched collection configuration. [2].

4-3 Comparison between Radial and Branched Topology

Due to the fact that radial and branched designs show the highest potential among all the aforementioned designs, only these two collection configurations will be treated. Both designs are suitable for the purpose of the current work, since they are cheaper compared to the other

two designs. This is very important for the optimization of the layout because the cable cost will be reduced and this will contribute to the reduction of the objective function.

In general, branched topologies are more preferable than the radial topologies. The main reason for this is the saving in total cable length that can be achieved from a branched topology compared to a radial one. This conclusion results from the fact that the global minimum cable length of a radial problem is part of the possible solutions of branching. Another advantage of branched topology is that a greater number of cable connections use lower rated and thus less costly cables.

In addition, by using branched topology the savings in terms of power losses are greater compared to radial topology. This occurs because the electrical losses in one cable are proportional to the square of the current that flows through the cable. Thus, for a cable that connects two turbines, the losses will be proportional to the square of the number of turbines upstream of that cable.

Finally, reliability of branched topology is another significant factor, which influence the choice of which of the two topologies to be implemented. In order to make this advantage more clear, Figure 4-6 is used. So, in case of radial topology and assuming that a cable fault occurs between 2 and 3 turbines, then the power coming from three upstream turbines is lost. However, in case of the branched topology, the cable fault between these turbines, then power will be lost only from these two turbines.

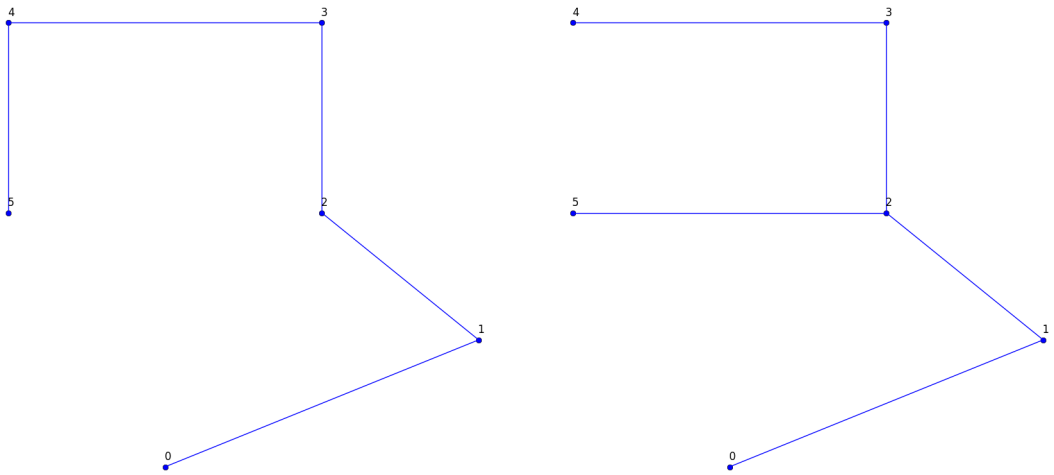

Figure 4-6: Branched collection configuration. [2].

4-4 Comparison between Single and Multiple Cables

In the more recent Offshore Wind Farms (OWF), multiple cable types are used instead of only one cable type. The main reason for this trend is that a significant cost reduction can be achieved. More specifically, by using multiple cables, the pointless use of a high capacity and thus expensive cable can be decreased and eliminated. Thus, this can contribute to the total cost saving.

Based on the previous argument, multiple cables are suitable for current work, since they contribute to the cable cost saving, which in turn will contribute to the decrease of the total investment costs. The decrease in investment cost is important for this Thesis, since it affects the result of the Levelized Production Cost (LPC), which is the objective function.

In Georgios Katsouris's project [2], three approaches have been examined so as to solve the Offshore Wind Farm Infield Cable Topology Problem (OWFICTP), where more than one cable type was used. These approaches are the following:

- High to Low Approach
- Low to High Approach
- Online Approach

After several steps of comparisons among the above three approaches, it has been found out that the Online approach is the best for the multiple cable types OWFICTP.

4-5 Offshore Wind Farm Infield Cable Topology Problem OWFICTP

In order to solve the Infield Cable Topology Problem for the radial connection of OWF, the Planar Open Savings (POS) Heuristic was used [2]. The POS heuristic has been developed by Bauer and Lasgaard [12] and it has two different versions, POS1 and POS2.

Apart from POS, RouteOpt local heuristic has been also developed by Bauer and Lysgaard [12] and it is used in order to improve the generated sub-optimal routes of POS1 and POS2. RouteOpt is applied to each individual route, but first the topology has been obtained by POS1 and POS2.

As it has already been mentioned in section 4-3, besides radial designs for the Infield Cable Topology (ICT) of OWF, also branched topologies are of great interest. Finding the optimal branched solution of the OWFICTP corresponds to the well defined Capacitated Minimum Spanning Tree (CMST) problem [13].

For the CMST problem another heuristic was developed named Esau-Williams (EW) Heuristic. EW gives more freedom and possibilities for merging of routes since there is no limitation on the position of the turbines in their corresponding routes. The main characteristic of EW heuristic is that it first tries to connect the turbines that are relatively further from the substation into clusters. After a cluster has been completed,meaning that the capacity of the cables is full, the algorithm continues with a different cluster, closer to the substation and so on [2].

4-6 Hybrid algorithm and Discussion

The Hybrid algorithm has been developed by G. Katsouris [2] in order to enhance the performance of EW when multiple cable types are used. Hybrid algorithm combines two algorithms, POS1 and EW and it tries to achieve branched routes by the inter-connection of the radial

routes. For that reason, Hybrid algorithm starts first using POS1 and cable capacity corresponding to the low capacity cable. Subsequently, the branched layout for multiple cable types is defined by using EW approach. The layout generated from POS1 is used as initial solution for EW. The final step is the implementation of RouteOpt in every radial part of the routes and only if the cheap cable is used. A more detailed description of the Hybrid approach is given in Appendix A.

In addition, G. Katsouris used a wide range of instances which simulated possible layouts of OWF in order to compare the performance of the algorithms. The results indicated two major distinctions:

- Use of single or multiple cables,
- The position of the substation inside (substation-in) or outside (substation-out) the wind farm.

In the current Thesis, multiple cables will be used, because their use can reduce significantly the cost, see section 4-4.

Regarding the multiple cables, G. Katsouris found the following results. In case of branched topologies, the Hybrid approach is better than EW algorithm. For radial layouts (POS algorithms), the cost performance was slightly better than POS1, but POS1 is significantly faster, mainly for the substation-out case. So, it is concluded that POS1 is the best choice, since its provided solutions are close to the corresponding solutions of POS2. Finally, the choice between POS1 and Hybrid algorithm depends on the substation position. In case that the substation is centrally located, the Hybrid approach gives better solution than POS1 in almost same computation time. In case of substation-out, Hybrid algorithm is better only when wide range of cable capacities are used, but the computation time required is too high compared to POS1. So, POS1 is the best option for the substation-out case.

In the current work, the substation will be centrally located. In that case, the length of the required cable between wind turbines and the substation will be smaller compared to the substation-out case. So, the cable cost will be also lower and it will contribute to a lower LPC value, which the objective function of the optimizer. In addition, for the substation-in case, the losses of the collection system are much less compared to the configuration where the substation is located outside. Thus, these are the reasons for which the substation-in is treated in the current work.

4-7 Cable Cost Model

The objective of this section is to express the cable cost in terms of capacity. The cable cost that will be used, includes cable procurement cost and cable installation cost. In addition, it should be noted that the additional cable length that extends from the seabed to the turbine's transformer and back down is not taken into account.

In order to calculate the cable procurement cost, the Lundberg's model is used by implementing the cable specifications from ABB [14]. The cost model of the AC cables is based on the

rated power of the cables. The equation that describes that model is presented in Equation 4-1 [15].

$$Cost_{AC} = A_p + \exp(\frac{C_p * S_n}{10^8}) \tag{4-1}$$

where:

- $Cost_{AC}$ is the cost of the AC cables [€/m]
- U_{rated} is the rated voltage of the cable, line to line [V]
- I_{rated} is the rated current of the cable [A]
- A_p, B_p, C_p are the cost constants
- S_n is the rated power of the cable [VA]

The rated power of the cable is given by Equation 4-2.

$$S_n = \sqrt{3} * U_{rated} * I_{rated} * \cos\phi \tag{4-2}$$

The power factor is assumed to be equal to 1.

In addition, the cost constants must be converted to the current values. Thus, an inflation rate of 1.18 for Sweden and an exchange rate of SEK to Euro of 0.083 are used [2].

The cost parameters A_p,B_p and C_p differ according to the magnitude of the rated voltage. The following Table 4-1 presents the cost parameters for AC cables, for different voltages [15].

Table 4-1: Cost parameters for AC cables, for different voltages

Rated voltage $[kV]$	A_p $[10^6]$	B_p $[10^6]$	C_p
22	0.284	0.583	6.15
33	0.411	0.596	4.1
45	0.516	0.612	3
66	0.688	0.625	2.05
132	1.971	0.209	1.66
220	3.181	0.11	1.16

Furthermore, in Table 4-2 the rated current of AC,XPLE 3-core,copper conductor cables is given according to the cross-sectional area[2]. Thus, by using Equation 4-1, rated voltage of the cable and the corresponding rated current the cable costs can be calculated.

Table 4-2: Cable procurement Costs

Cross section (mm^2)	Current Rating (A)
95	300
120	340
150	375
185	420
240	480
300	530
400	590
500	655
630	715
800	775
1000	825

Finally, cable installation costs must also be taken into account. They consist of transportation and laying costs. The aforementioned costs are usually given as a linear function of cable length and in some cases, the fixed costs are separated by the variable costs [16], [1]. For the current thesis, the cable installation costs are assumed to be equal to a fixed value of 365 €/m, as given in [17], which is of good order of magnitude compared to the 2400 SEK/m in [15].

4-8 Parameters

The inputs of the Offshore Wind Farm Infield Cable Topology Problem, OWFICTP, are the coordinates of the initial positions of the wind turbines inside the OWF, the coordinates of the substations and the cable capacities and cable costs. In addition, the type of the wind turbine, that is going to be used in the OWF, is of great importance since according to the rated power, the current rating is being calculated and then the cable cost is determined.

4-8-1 Position of Substation

The position of substation is also of great importance, since it is a parameter that affects a lot the final outcome. The substation can be located either inside the OWF or outside of it. In the current work, the substation is located in the center of the area defined by the existing turbines, see 4-6.

In order to find the position of the substation the following process is used. Initially, all the x coordinates of all wind turbines are added together and all the y coordinates of all wind turbines are added together. Then, both sums of x and y coordinates are divided by the number of the wind turbines. The result of these deviations provide the x and y coordinates of the substation. Regarding the calculation of the substation water depth, Equation 5-1 from section 5-2 is used.

4-8-2 Cable Capacity

Cable capacity is another parameter that must be defined. In the current thesis multiple cable types and combination of the cable capacities are going to be used. Based on the review of cable specifications [14], in most of the OWF 5 to 10 turbines are connected in a feeder. For multiple cables any combination of the cable capacities in the above range could be used. In the current work two cable types will be used. More specifically, the user can select two cable types of the same rated voltage from Table 4-1, but of different rated current, Table 4-2.

4-8-3 Type of Wind Turbine

Another very important parameter is the type of the wind turbine. Having different type of turbine leads to different current ratings, cable capacities and as a result to different cable cost. This can be seen from Equation 4-2.

From Equation 4-2 it is clearly observed that the current rating depends on the type of the wind turbine and the rated voltage. The user is able to select the type of the turbine inside from the code.

Lastly, the user has also the possibility to select which cable capacities to use according to the total number of turbines inside the OWF.

Chapter 5

Offshore Wind Farms (OWF) Support Structure

This chapter gives an overview of the support structures for Offshore Wind Turbines (OWT). First, an introduction for the support structures is provided and then a description of the MZ Tool follows. In addition, the water depth calculation for each wind turbine inside the OWF is presented.

5-1 Introduction

Offshore support structures and foundations for offshore wind turbines are proposed and delivered using a range of solutions. Both the advantages and disadvantages of each design concept are difficult to assess in a comparative and fair way. The designer of the support structures has to consider a number of issues in order to provide an appropriate solution. These factors are led by both the project and the external environment and include, [18]:

- Depth of the water column
- Mass needing support
- Turning and bending forces on the structure
- Location specific issues such as wind, wave, tidal and current considerations
- Seabed geology and soils
- Scour and sediment movement
- Environmental impact
- Construction requirements

- Installation requirements
- CAPEX
- OPEX
- Decommissioning
- Materials

In addition, the support structures for large offshore wind farms can be categorized into two main categories: grounded and floating designs. Both aforementioned support structure types can be further differentiated by their layout, the selection of their construction materials, method of installation and of course by their structural configuration.

Subsequently the support structures can also be sub-categorized in six types according to the structural configuration. These six sub-categories are the following, [18]:

- Monopile Structures
- Tripod Structures
- Lattice Structures
- Gravity Structures
- Tripile Foundation
- Floating Structures

In the following Figure 5-1, the various support structure types are illustrated.

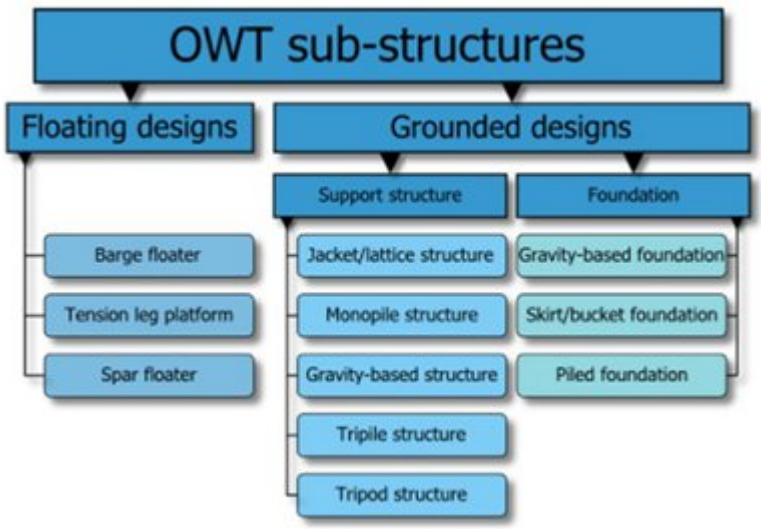

Figure 5-1: Categories and sub-categories of OWT structures. [18].

In the current work, monopile support structure was used for all the OWT inside the OWF.The monopile support structure is a relatively simple design by which the tower is supported by the monopile. Tower and support structure can be connected either directly or via a transition piece. In most Offshore Wind Farms with monopile support structures the second design is more used. Monopiles are currently the most commonly used foundation in OWF due to their ease of installation in shallow to medium water depths. This type of support structure is usually used for water depths between 0 and 30 meters.

In Figure 5-2 an overview of monopile support structure is illustrated.

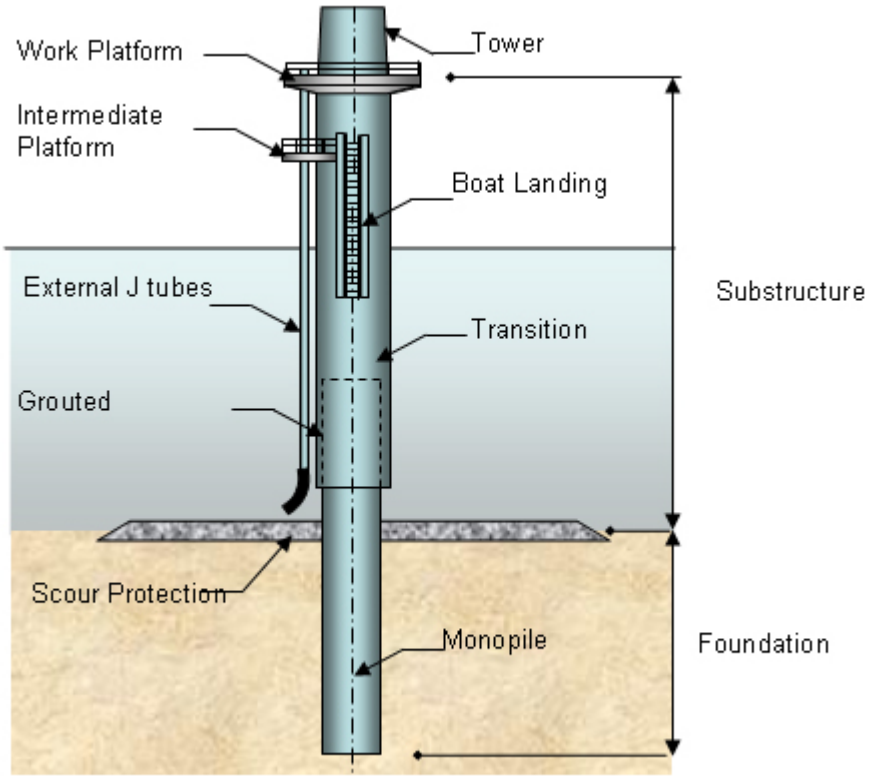

Figure 5-2: Overview of monopile support structure. [19].

5-2 Water Depth Calculation

Support structure is very important for the wind farm layout, because it is interlaced with another variable that does have a relation with layout: the area of the development. Water depth is one of the main drivers of support structure design; too shallow or too deep waters are avoided, due to inaccessibility and cost.

More specifically, water depths outside the range of 2 meters to 30 meters are not usually considered for an offshore wind farm, although it is technically feasible to place turbines outside this range.

Another quite important variable is seabed conditions since depending on these conditions the more suitable support structure for the site is going to be used.

As it has already been mentioned, monopile support structures are going to be used for the current MSc Thesis. In addition, the seabed is considered to be a linearly sloped surface plane. The water depth is also of great importance, since the deeper the wind turbines are going to be placed the more expensive they will be. A direct consequence of their high costs is the increase of the total investment costs, which in turn leads to the increase of the Levelized Production Cost (LPC).

In order to calculate of the water depth of each wind turbine inside the Offshore Wind Farm, it is assumed that three points inside the site are known. That means that the coordinates x,y and z for three wind turbines are known. Then, by using the linear algebra and specifically the determinant of the three known points, the equation of the seabed is defined. The seabed is a $3D$ linearly sloped surface plane and its equation is given by the following formula:

$$\begin{aligned} z = &((y - y_1) * ((x_2 - x_1) * (z_3 - z_1) - (x_3 - x_1) * (z_2 - z_1)) \\ &- (x - x1) * ((y_2 - y_1) * (z_3 - z_1) - (z_2 - z_1) * (y_3 - y_1))) \\ &/((x_2 - x_1) * (y_3 - y_1) - (y_2 - y_1) * (x_3 - x_1)) + z_1 \end{aligned} \tag{5-1}$$

where:

- z is the water depth of a specific point inside the wind farm,
- x,y correspond to the coordinates of the specific point mentioned above,
- x_1, y_1, z_1 is the first known point in the farm,
- x_2, y_2, z_2 is the second known point in the farm and
- x_3, y_3, z_3 is the third known point in the farm.

Thus, by inserting each time the coordinates of all wind turbines inside the algorithm as an input, their water depth can be easily calculated by this equation.

Furthermore, it is of great importance to be mentioned that the seabed equation is defined inside a Python function which means that the user can easily change the shape of the seabed depending each time on the data that the user has.

Finally, a $3D$ plot of the seabed and the positions of the wind turbines inside the site has been created.

5-3 The MZ Tool

The MZ tool has been developed by Professor Michiel Zaaijer of the Delft University of Technology[1].

In the current work, only a part of the whole MZ tool has been used. More specifically, only the algorithm corresponding to the support structures was used. Thus, the aerodynamic

loads, hydrodynamic loads, dimensions of the components of the support structure, the mass of each component and the stresses in both the tower and the support structure of each wind turbine were all calculated with the help of the MZ tool algorithm. In addition, the cost model for the support structures will be also taken by the MZ tool.

Chapter 6

Analyzer Results and Case Study Description

This chapter provides the results derived from the combination of wake effects, cable topology and support structure variation. These results are the cable cost and length, the annual energy yield, the support structure cost, the investment cost, the O&M cost, the decommissioning cost and the Levelized Production Cost (LPC). For the performance of the analyzer, the layout of the Horns Rev 1 Offshore Wind Farm (OWF) will be used for a case study. The purpose of this case study is to prepare the 3 analyzer ingredients and test their suitability for the optimizer described in the next chapter.

6-1 Description of the Case Study: Horns Rev

The Horns Rev Offshore Wind Farm compromises of 80 wind turbines capable of producing 160 MW. This farm is located in the North Sea 14 kilometers west of Denmark, see Figure 6-1. Horns Rev was the world's largest offshore project when it was installed in 2002. Horns Rev uses Vestas $V80{-}2MW$ turbines, which have an $80m$ rotor diameter. The total area of the site is approximately $20km^2$ [20]. The distance between two wind turbines is $560m$.

Figure 6-1: Location of the Horns Rev OWF.

Figure 6-2 illustrates the position of each turbine inside the Horns Rev wind farm. In Table C-3 in Appendix C the coordinates of the wind turbine positions can be found.

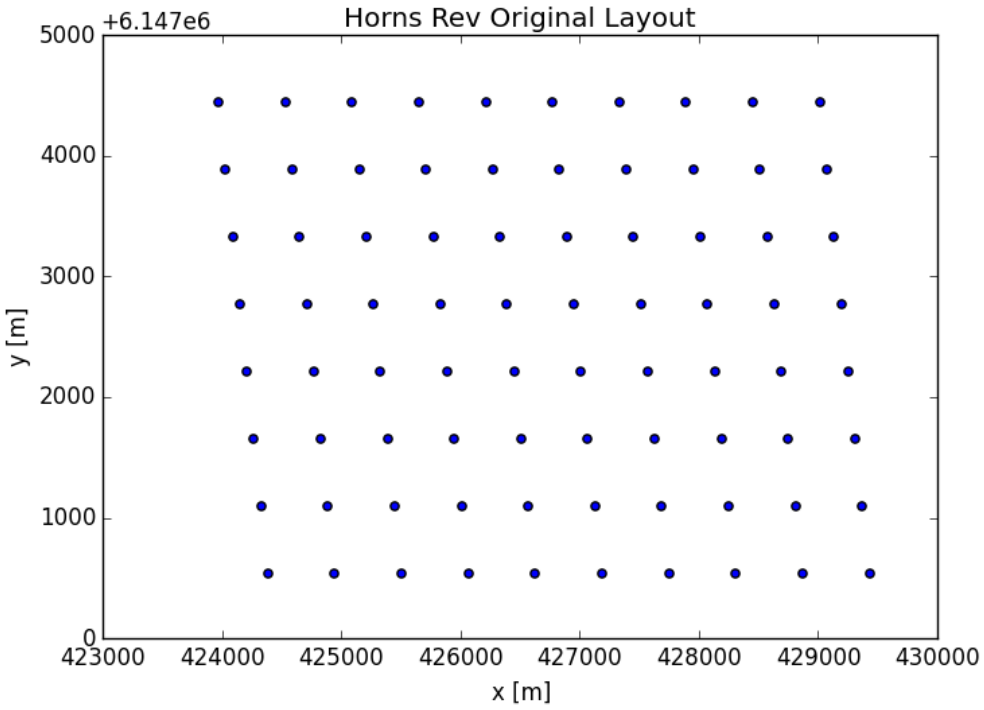

Figure 6-2: Original OWT locations for Horns Rev site.

Based on the existing data for the Horns Rev OWF (section 6-2) and on the algorithms

mentioned in the previous chapters, the wake effects and the support structure variation combined in one single algorithm. Regarding the cable topology, the analyzer uses the Hybrid approach, mentioned in subsection 4-6, instead of the real cable topology of the Horns Rev I OWF.
From the analyzer algorithm, the Levelized Production Cost, the annual energy yield, the water depth of each turbine, the support structure costs and the infield cable cost and length can be calculated.

6-2 Analyzer Inputs

The inputs that are used in the aforementioned algorithm can be seen below:

- Layout of the wind turbines. At first, the layout of the Horns Rev wind farm is used, but this is going to be changed with the help of the optimization tool described in section 7,
- Site conditions. The site conditions differ from site to site and they can have a great impact on the final result,
- Wind turbine characteristics. The most important characteristics are the power and the thrust curve,
- Electrical system data. These data are the position of the substation, the rated voltage and the current capacity of the cable, the length of the transmission cable and the distance to grid,
- Wind rose. The user can change the degrees of the wind direction bins,
- The shape of the seabed. It is already mentioned how the seabed shape is defined and how the user can change it in section 5-2,
- LPC parameters such as interest rate, inflation rate and the operational lifetime.

6-3 Analyzer Results

In the following subsections the results of each ingredient in the analyzer are presented. It must be noted that the results can be trusted, since all the used algorithms/tools were tested and verified in the corresponding Theses.

6-3-1 Wake Effects Results

As it has already been mentioned, the algorithm developed in [4] is used for the wake effects. In that algorithm, the Jensen wake model was run with wind roses with wind direction bins of 1 degree and 30 degrees.

However, in the current work a different value is used. There are two reasons for this change. First, in case of the 1 degree the computation time is too large, which is not desirable because

during the optimization process the computation time will be even higher. Secondly, the case of the 30 degrees is not used because this wind direction bin is large and may cause inaccuracy of the results. For these reasons, the analyzer was run 6 times with different wind roses, in terms of the wind direction bin, so that the most suitable one could be selected.

It must be noted that a random layout of 80 wind turbines was selected for these runs.

From all the above, Figure 6-3 was found. This Figure illustrates the LPC values versus the different wind direction bin sizes. It can be seen that for each wind direction bin smaller than 10 degrees the LPC has almost the same value and the line becomes asymptotic towards axis-x.

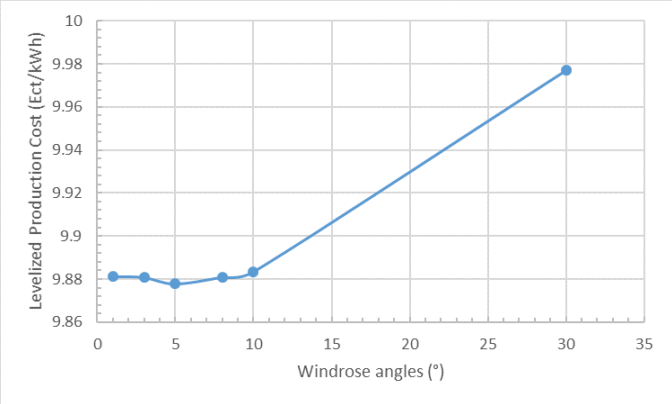

Figure 6-3: LPC values for wind direction bins.

Finally, taking also into account the computation time, Figure 6-4 was created for the same layout. This Figure depicts the same LPC values as above, but now versus the computation time. The computation time refers to the time that the analyzer required for different wind direction bin sizes.

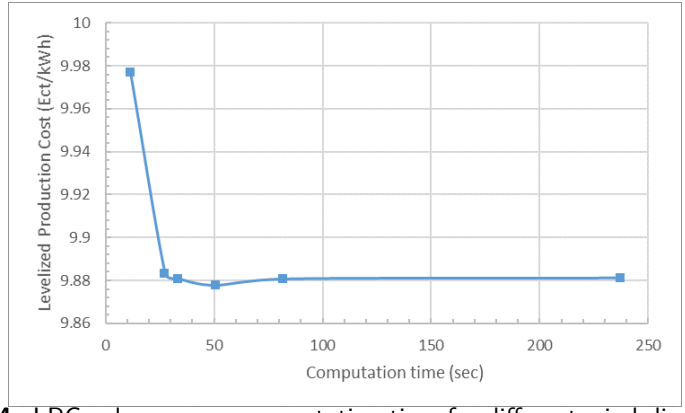

Figure 6-4: LPC values versus computation time for different wind direction bins.

From Figure 6-4, it can be seen that the lower the wind direction bin is, the higher the computation time is.

Taking into consideration both Figures, a wind direction bin of 8 degrees was selected.

6-3-2 Cable Topology and Cable Cost

As far as the infield cable is concerned, two cable types of $33kV$ each were selected. In addition, the selected rated current was $420A$ and $655A$ respectively. By having these inputs and the cable cost model described in section 4-7, the capacity, expressed in terms of the wind turbine number that can be connected in a feeder, was found to be 6 and 10 for these two cable types. Figure 6-5 illustrates the cable topology for the Horns Rev site after the implementation of Hybrid algorithm. Apart from the cable topology, this Figure shows the two different cable types that were used.

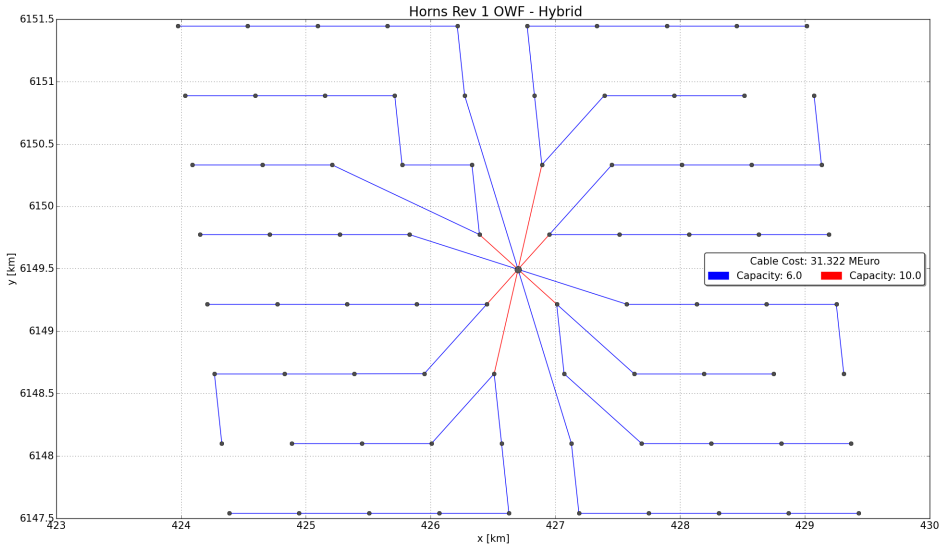

Figure 6-5: Hybrid - Horns Rev - Substation in.

From Figure 6-5 it can be observed that the cable topology for the Horns Rev 1 OWF is different compared to the existent cable topology, see Figure 6-6. However, that was expected, since the Hybrid algorithm tries to find the best cable topology in terms of lowest cable cost and cable length.

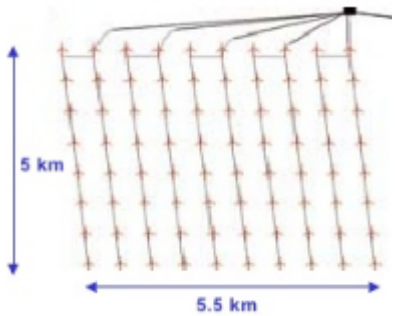

Figure 6-6: Existent cable topology of Horns Rev 1[21].

For the current case study, the cable cost and the cable length are equal to $31.322M€$and

49.313km respectively. On the other hand, the cable length of the existent cable topology is equal to 63km[18], which makes Hybrid algorithm suitable for the current work.

In addition, the sensitivity of the Hybrid algorithm is examined so that the suitability of this algorithm for the current project will be tested. In order to do that, two wind turbines of the existent Horns Rev 1 topology are selected and they are moved 12 times each. By doing that, it can be seen how sensitive the algorithm to these changes is and how the cable topology, cable cost and cable length are affected.

The two wind turbines that are going to be moved are the following:

- The wind turbine in the 5^{th} row and 3^{rd} column from the left to right (Figure 6-5),
- The wind turbine in the 5^{th} row and 4^{th} column from the left to right (Figure 6-5).

The exact coordinates of these wind turbines can be found in the corresponding Table of Appendix C. The corresponding serial numbers of these wind turbines are 21 and 29. It must be mentioned that the 21^{st} turbine has an ascending direction to the right while the 29^{th} turbine has a descending direction to the right. More specifically, both x and y coordinate of the 21^{st} turbine are increased until the point that the turbine will be almost between the third and fourth turbine of the fourth row, see Figure 6-5. Regarding the 29^{th} turbine, the y coordinate of that turbine is decreased while its x coordinate is increased, see Figure 6-10.

After 12 instances for each wind turbine position, the following Figures were found.

Figure 6-7 illustrates the change in the cable cost according to the turbine positions for both 21^{st} and 29^{th} wind turbines.

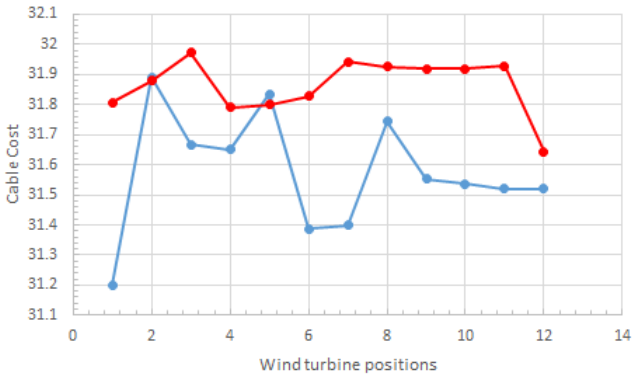

Figure 6-7: Cable cost versus wind turbine positions for both 21^{st} (blue line) and 29^{th} (red line) turbines.

Figure 6-8 illustrates the change in the cable length according to the turbine positions for both 21^{st} and 29^{th} wind turbines.

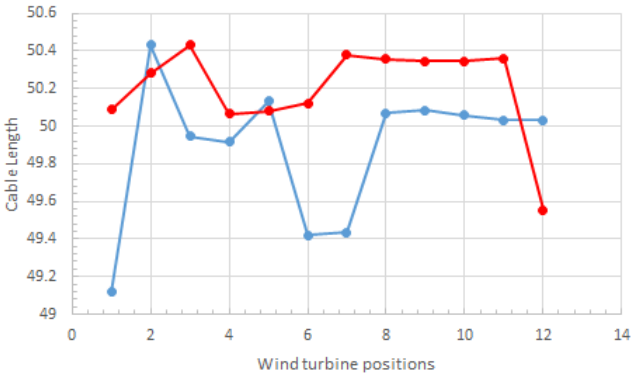

Figure 6-8: Cable length versus wind turbine positions for both 21^{st} (blue line) and 29^{th} (red line) turbines.

From Figure 6-7 and Figure 6-8, it can be observed that the Hybrid algorithm has high sensitivity, since changing the position of only one wind turbine inside the farm then the algorithm tries to find the new most cost effective topology. That means that if a wind turbine position is changed the cable routes around this turbine will change as well. As a result both cable cost and cable length will be changed.

It should be noted that for a removal of one wind turbine, the cable topology changes. In addition, the change in turbine position will change the way the two cable types will be used. This behavior is observed both for the turbine far from the substation (blue line) and close to the substation (red line).

Figures 6-9 and 6-10 illustrate the new cable topology of the wind farm after 12 removals for each turbine. The circled turbine is the final position of the the turbines after 12 removals.

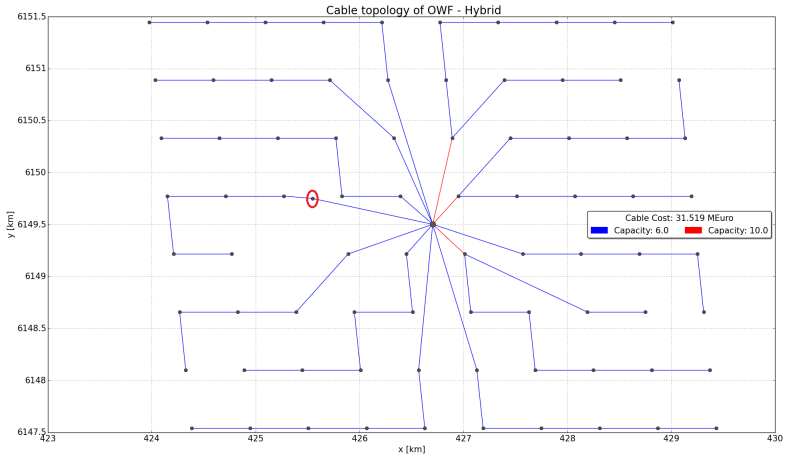

Figure 6-9: Cable topology after 12 removals of the 21^{st} turbine.

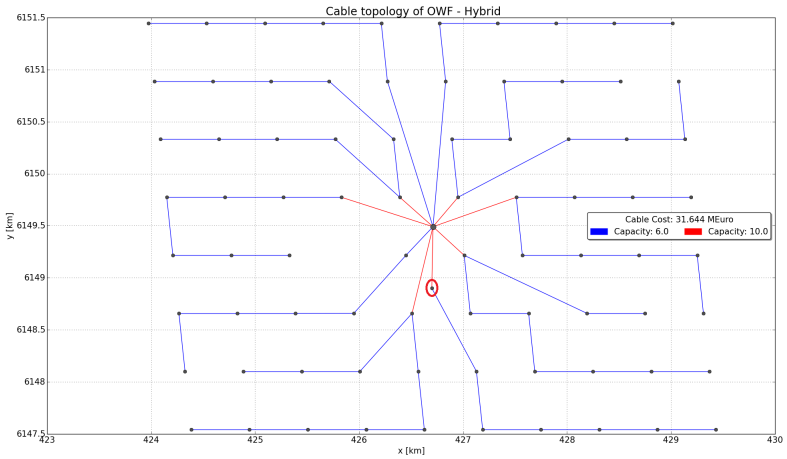

Figure 6-10: Cable topology after 12 removals of the 29^{th} turbine.

As it was expected the cable routes around these two wind turbines have been changed. In the first case the cable cost is $31.519M€$while the cable length is equal to $50.032km$. In the second case the cable cost and the cable length are equal to $31.644M€$and $49.554km$ respectively. It can be seen that the removal of the wind turbine closer to the substation causes an increase to the cable cost, but a decrease to the cable length. This may be due to the fact that changes closer to the substation affect more the way the two cable types will be used.

The high sensitivity of the Hybrid algorithm makes this algorithm suitable for the objective of the current work. Specifically, during the optimization, the optimizer will try to find the best layout, which means that each time that the positions of the wind turbines change, then the Hybrid algorithm will find the most cost effective cable topology.

6-3-3 Seabed and of the Support Structure Cost

As it has already been mentioned in section 5-2, three points inside the site are considered as known, so that the shape of the seabed can be defined. For the Horns Rev 1 case the known points can be seen in Table 6-1. The x and y represent the coordinates of the wind turbines inside the farm. The fourth column of the table corresponds to the water depth of each point.

Table 6-1: Definition points for the seabed shape

No.	x [m]	y [m]	z [m]
1	423974	6151447	6
2	429431	6147543	14
3	424386	6147543	6.5

In addition, the seabed for the current case study is assumed to be a linearly sloped surface

plane, see section 5-2. For a better understanding, Figure 6-11 illustrates the shape of the seabed and the positions of the offshore wind turbines as well.

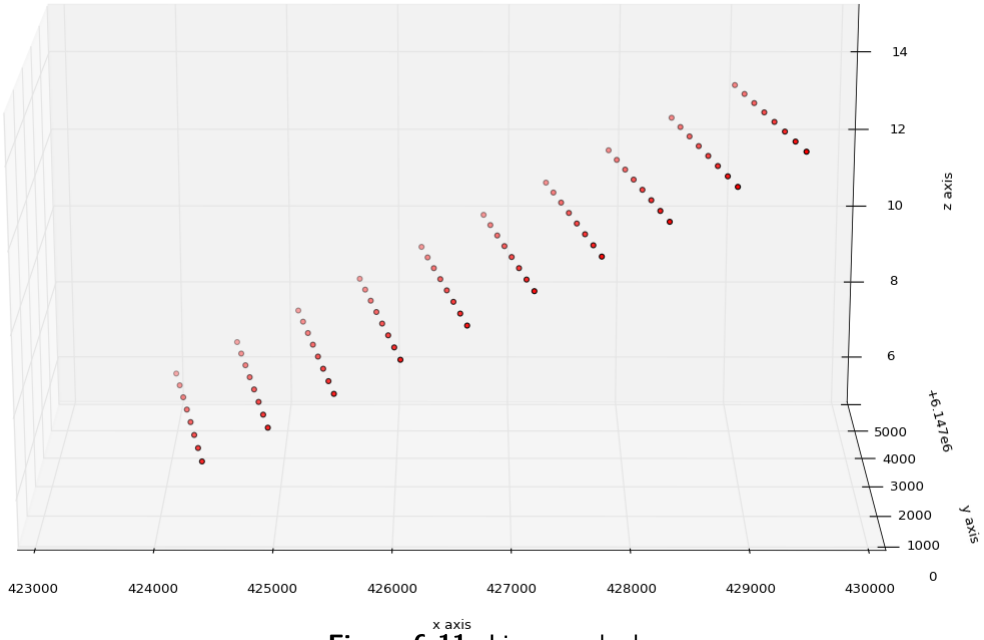

Figure 6-11: Linear seabed.

Concerning the support structure cost, each monopile support structure is different for each wind turbine, since the foundations are dependent of the water depth. Thus, based on the current seabed shape and the cost model of MZ tool [1] derived that the support structure cost for the whole Horns Rev farm is 131.629$M€$.

The aforementioned support structure cost is considered high compared to the real support structure cost of Horns Rev 1 (75$M€$[1]), which use one design of support structure. Thus, more research has been done so that the reliability of the analyzer will be examined. So, the analyzer was tested for a fixed water depth, which means that all the wind turbines will have the same design for the support structure. The maximum value of the water depth (14 meters) was used for this case so that all wind turbines can withstand extremes of wind speed and storm waves.

After the implementation of the analyzer, it was found that the total support structure cost is equal to 117.931$M€$. That is not as expected in the first place, since it was expected that the support structure cost will be higher when the maximum water depth is used for the support structure design for all wind turbines.

So, further research in the input value of the wave height will be done since the wave loading plays important role to the design of the support structure.

More specifically, the costs of support structures for water depths between 6 and 14 meters are determined and presented in Figure 6-12. This Figure illustrates the change in the support structure cost according to the water depth.

It must also be mentioned that waves are limited to the braking wave height and the wave height values that were used in the analyzer are:

- $H_{s,50years} = 5.0m/s$
- $H_{s,1year} = 0.64 * H_{s,50years} = 3.3m/s$

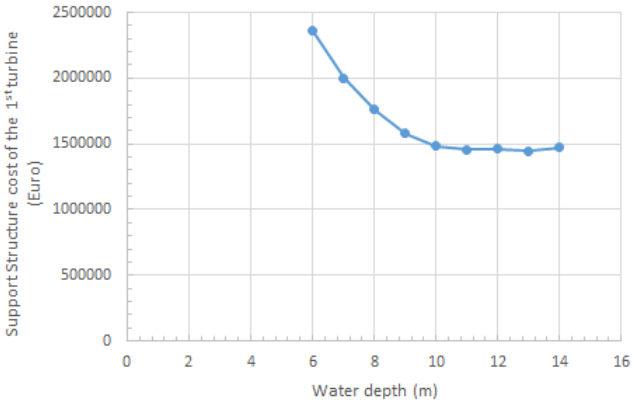

Figure 6-12: Support structure cost for different water depths.

Afterwards, the costs of the support structure for the same range of water depth, but for lower wave height values were determined. For these instances the wave height values are:

- $H_{s,50years} = 0.1m/s$
- $H_{s,1year} = 0.05m/s$

These low wave height values were selected so that the affect of the wave height can be examined compared to the high values of the first case.

The output of these instances is Figure 6-13, which illustrates again the support structure cost versus the water depths.

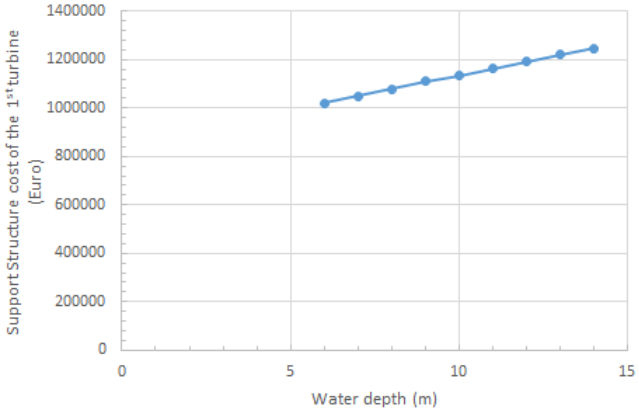

Figure 6-13: Support structure cost for different water depths.

From the Figures above, it can be clearly concluded that the wave height affects a lot the design of the support structure and as a consequence the support structure cost. Using high wave height values, as in the first case, the support structure cost is smaller in deeper waters. This happens because with high wave height, the wave loading is increased. That is the explanation why the total support structure cost was lower when the 14 meters water depth was used as a fixed value for all the wind turbines. So, in case of a fixed water depth value, 6 meters would be the ideal value, since the most expensive support structure is found at that water depth. Specifically, the 6 meters water depth is the ideal value, because if all wind turbines use the support structure design of that water depth then they will be able to withstand extremes of wind speed and storm waves.

On the other hand, when low wave height values are used then the support structure cost increases as the water depth increases. From Figure 6-13, it can be seen that the support structure cost increases linearly with the water depth.

For the current work the first case will be examined, namely the one with the high wave height. In reality, this is a common case, since the support structure cost does not depend only on the water depth, but there are also other factors that play important role for the design of the support structure such as the wave height. With that wave height value the support structure cost will be decreased in deeper waters and after 9 meters water depth it becomes almost the same, see Figure 6-12. In addition, the optimizer will try to find the best layout in deeper waters where the support structure costs are lower.

6-3-4 Levelized Production Cost

In order to calculate the LPC, Investment, $O\&M$ and Decommissioning costs must be determined. Based on the cost models described in section 2 and by implementing the analyzer algorithm, all the aforementioned costs for the Horns Rev 1 case are calculated and provided in Table 6-2.

Table 6-2: LPC costs

Investment costs [$M€$]	$O\&M$ costs [$M€/y$]	Decommissioning costs [$M€$]
431.6	25.142	57.774

The high investment cost of the support structure contribute significantly to the total investment cost of the farm and that is the reason why this cost is high. The investment cost of the piles is high because many of the wind turbines in Horns Rev 1 are placed in waters where the water depth is lower than 9 meters, see Figure 6-12. These costs are considered high compared to the real data of the Horns Rev 1. More specifically, the real investment costs are equal to $337M€$[1].

As a consequence the operation and maintenance cost is also high, since it is equal to 6% of the total investment cost. In addition, the decommissioning cost is relatively high for the same reason like the investment cost.

Another very important parameter of the Levelized Production Cost is the annual energy yield, which equals to $693GWh$ for the current case study, see subsection 6-3-1. Finally,

having all the above, the total LPC for the Horns Rev case is equal to 9.848 €ct/KWh. These both values are also higher compared to the corresponding real values which are equal to 600GWh and 7.11€ct/KWh respectively[1].

Chapter 7

Optimization algorithm and selected parameter settings

This chapter provides an overview of the optimization tool. Furthermore, different case studies are going to be tested in this chapter so that the performance of the optimization tool will be examined. All these scenarios are demonstrated in the following sections.

7-1 Description of the Optimization Algorithm

As it has already been mentioned, the current work consists of two parts. The first part was the analyzer described in section 6 and the second and more interesting part is the development of an optimization tool based, of course, on the analyzer.

There are several ways/algorithms for optimization. In the current work, the Genetic Algorithm (GA) is used. In general, a genetic algorithm is a search heuristic that mimics the process of natural selection. This specific heuristic is extensively used to generate useful solutions to optimization and search problems. In addition, genetic algorithms belong to a larger class of evolutionary algorithms (EA), which generate solutions to optimization problems using techniques inspired by natural evolution, such as inheritance, mutation, selection and crossover.

In a genetic algorithm, a population of candidate solutions, called individuals, to an optimization problem is evolved toward better solutions. Each individual has a set of properties that can be mutated and altered.

For a genetic algorithm, the evolution starts from randomly generated individuals. This is an iterative process and in each iteration the population is called generation. Furthermore, in each one of these generations, the fitness of every individual in the population is evaluated. The fitness is, in other words, the objective function in the optimization problem being solved. In the current work, the objective function is the Levelized Production Cost (LPC), which is going to be minimized. The more fit individuals (called parents) are selected from the current

population and then they are recombined and randomly mutated to form a new generation. Afterwards, that new generation of candidate solutions is then used in the next iteration of the algorithm.

As far as the recombination is concerned, the user has to select a number of parents and these parents will give birth to new individuals. The number of these new individuals will be equal to the total population minus the selected number of the parents. Each individual is generated by using 2 parents and all parents contribute to the creation of the new individuals. The process described above takes place in every generation.

In addition, another important process of the GA is the mutation and it takes also place in every generation. The purpose of the mutation is to avoid a possible local optimum. For that reason, the user have to choose a mutation percentage, which indicates how many individuals of the current population will be replaced by random ones. It must be noted that the best individual of each generation is excluded from the mutation process.

There are two most commonly used algorithm terminations. Either after a specific number of generations or when a satisfactory fitness level has been reached for the population. For the current work the first type of termination is used.

Once the genetic representation and the fitness function are defined, a GA proceeds to initialize a population of solutions and then to improve it through repetitive application of the mutation, crossover, inversion and selection operators.

Figure 7-1 illustrates the flowchart of a genetic algorithm.

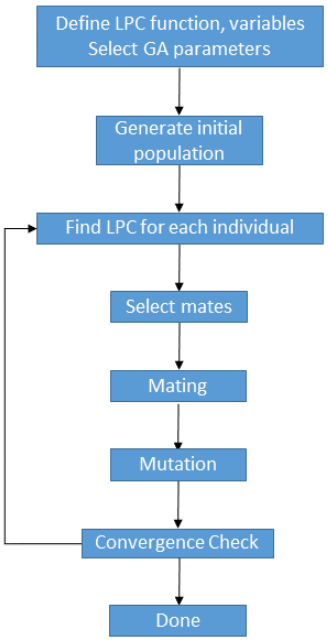

Figure 7-1: Flowchart of a GA.

As far as the GA parameters are concerned, the user can easily modify them through the code. These parameters are the number of the generations, the number of the population and the number of the most fit individuals. Moreover, it must be noted that if only a few individuals are selected, the algorithm would very rapidly converge to a local optimum, without a wider exploration of the solution space. Finally, although the number of turbines is not a direct parameter for the genetic algorithms, it is of great importance for the current optimization tool, since it affects the layout of the farm.

7-2 Wind farm layout concept

There are several approaches in order to map the wind farm layout into design variables. In the present MSc Thesis a structured and regular pattern for the wind turbines is defined. This can be done by using a structured grid, as rows and columns with fixed spacing. Thus, each square of the grid will correspond to one wind turbine position. As a consequence of that, the number of necessary design variables can be reduced significantly.

7-2-1 Position Constraints

Two types of position constraints are taken into consideration in this work; the wind turbine position inside the boundaries of a region and the relative position of two wind turbines inside the farm.

7-2-2 Region Boundaries

Due to the fact that there are several external factors that can limit the possible locations of the wind turbines in the wind farm optimization process, it is necessary to be able to constrain the possible position of the wind turbines. Some of these limitations are protected areas, ship routes, bird migration path and etc.

In addition, the boundaries of the region for the current work will be defined by a polygon. The advantage of the structured grid is that the wind turbine positions are automatically bounded inside the polygon domain. There is therefore no need to use a constraint on the wind turbine position.

For the current work, the polygon is a rectangular area which is bounded by four points with x and y coordinates. More specifically, x_{min}, y_{min}, x_{max}, y_{max} coordinates from these 4 points are required to define the rectangular. Then, the user has to define the number of the possible wind turbine positions inside that polygon and the step between them. The step between these positions must be defined for both x and y axes and it is the distance between 2 possible positions. These steps are given by the following equations:

$$\text{For x axis: } stepx = \frac{x_{max} - x_{min}}{x_n - 1} \tag{7-1}$$

$$\text{For y axis: } stepy = \frac{y_{max} - y_{min}}{y_n - 1} \tag{7-2}$$

where x_n and y_n correspond to the number of possible wind turbine positions in x and y axis respectively.

In order to check whether these steps are valid, the user must define the minimum distance d between two wind turbines, see subsection 7-2-3. If *stepx* and *stepy* are larger than the distance d then both steps are valid and the grid is defined. Afterwards, the user can select the number of the wind turbines that he wants to have inside the grid. For each wind turbine the serial number and the coordinates are defined.

In the following Figure 7-2, the discretization of the area with different spacing is illustrated.

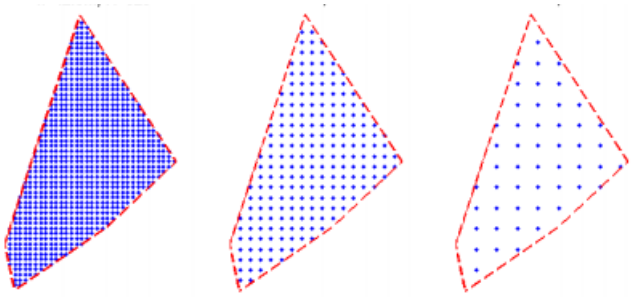

Figure 7-2: Discretization of the area with different spacing [22].

Using this approach, the user can easily change the number of rows and the number of columns, if for example he/she wants to have a more denser grid, which means to have more possible positions for the wind turbines.

It should be mentioned that in this project the rectangular is defined in such a way that the range of water depth is approximately between 6 and 14 meters. However, this range can be easily changed/controlled by changing the coordinates that define the rectangular.

7-2-3 Minimum Distance between Wind Turbines

Regarding this constraint, there is a minimum distance, under which two wind turbines are too close to each other to operate under normal conditions. It is not recommendable for two wind turbines to be closer than one rotor diameter. Thus, this constraint must be taken into account so that unrealistic solutions will be avoided.

For the current Thesis, the minimum distance between two wind turbines is assumed to be one rotor diameter plus a safety margin of $20m$.

It must be noted that the user can control the spacing between the possible locations in the structured grid. Thus, the distance between the wind turbines can be controlled.

7-3 Study of genetic algorithm parameter settings

In order to examine the performance of the optimization tool, it will be tested for different values of some of its parameters, mentioned in section 7-1.

7-3-1 Introduction to the scenarios

For the performance of the current optimization tool, four different scenarios are examined and they are presented below:

- Use of 30 parents, 15 generations and 80 wind turbines,
- Use of 10 parents, 15 generations and 80 wind turbines,
- Use of 30 parents, 20 generations and 30 wind turbines,
- Use of 10 parents, 20 generations and 30 wind turbines

For all the aforementioned scenarios, a linearly sloped surface plane is used as seabed. Each wind turbine has its own water depth and all the calculations related to the support structures are using the corresponding water depth. Furthermore, both wakes effects and cable topology are calculated as it has already been described in previous chapters.

As it has already been mentioned in subsection 2-2-2, a fixed value for $O\&M$ costs is used for all generations. This value is equal to the average value of all $O\&M$ values calculated for each individual in the initial population.

In addition, the initial population for all scenarios is equal to 50, which means that the initial population consists of 50 different layouts.

It must also be mentioned that each scenario was tested more than once for validation of the results, since the initial population generated by the genetic algorithm is random.

7-3-2 Scenario 1

In the first scenario, 30 parents and 80 wind turbines were used. The genetic algorithm ran 9 times for this case and the average computation time of each run was equal to 15645.326 seconds or 4 hours and 21 minutes.

The genetic algorithm for this specific scenario uses 15 generations. For each generation, the best offshore wind farm layout, in terms of the lowest Levelized Production Cost, is kept until the GA finds a lower LPC than the one of the previous generation.

Figure 7-3 illustrates the LPC values of the best layouts of each generation for all 9 attempts of the genetic algorithm.

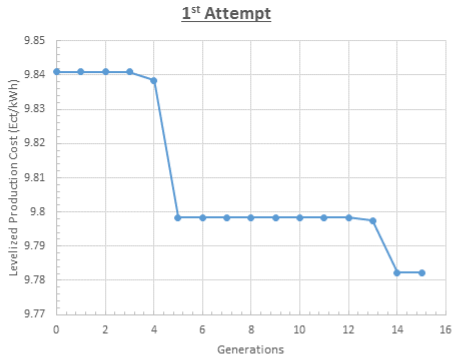
1st Attempt
Levelized Production Cost (Ect/kWh)
Generations

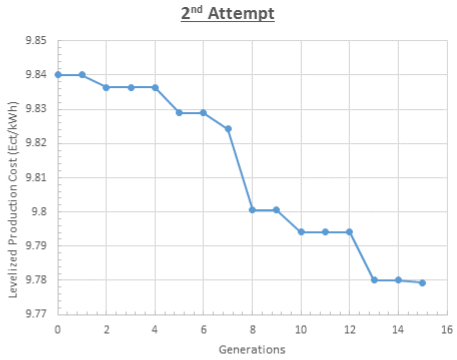
2nd Attempt
Levelized Production Cost (Ect/kWh)
Generations

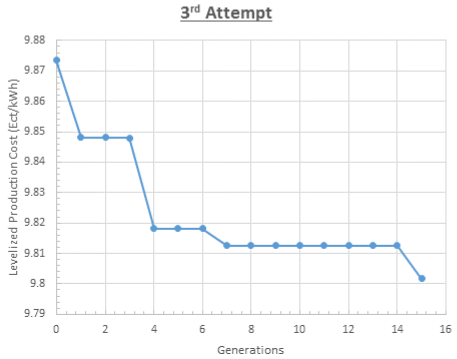
3rd Attempt
Levelized Production Cost (Ect/kWh)
Generations

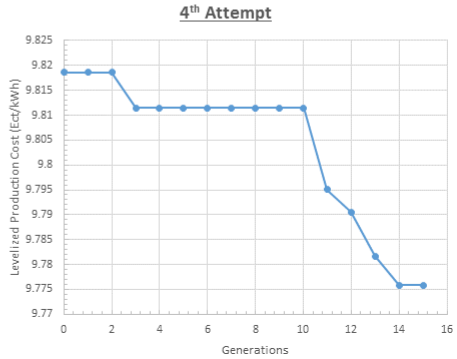
4th Attempt
Levelized Production Cost (Ect/kWh)
Generations

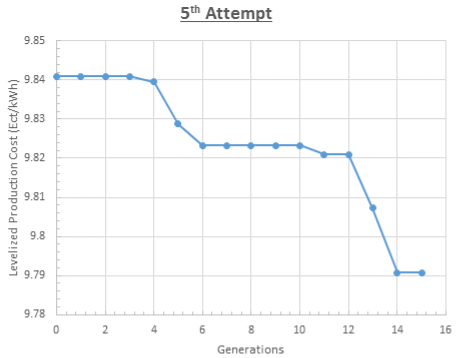
5th Attempt
Levelized Production Cost (Ect/kWh)
Generations

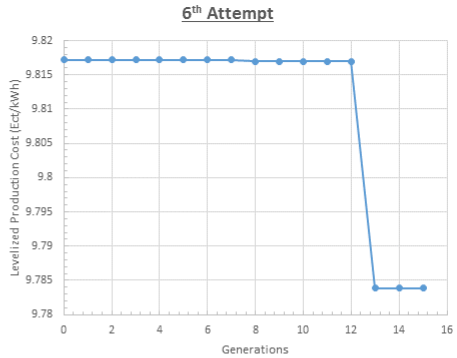
6th Attempt
Levelized Production Cost (Ect/kWh)
Generations

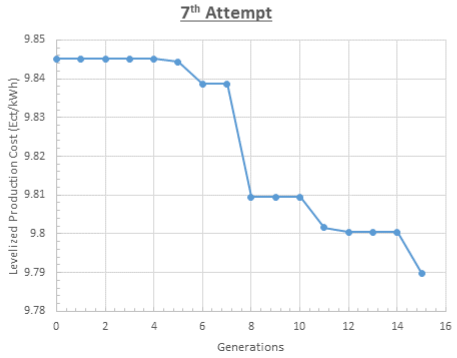
7th Attempt
Levelized Production Cost (Ect/kWh)
Generations

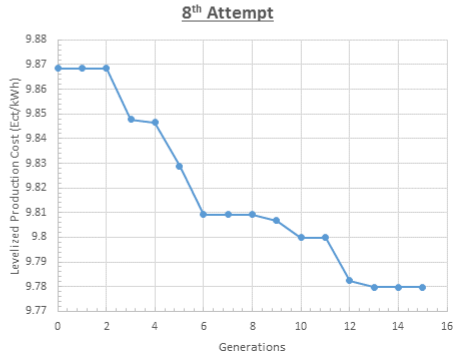
8th Attempt
Levelized Production Cost (Ect/kWh)
Generations

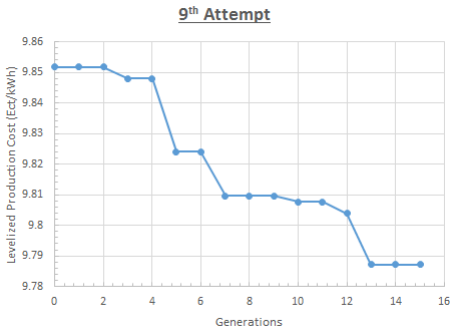

Figure 7-3: Levelized Production Cost [€ct/KWh] versus number of generations for the first scenario.

From the graphs of Figure 7-3, it can be seen after 15 generations the LPC is going to get approximately the same value in each attempt. However, the way that the LPC value decreases in each attempt is different. This occurs due to the fact that the initial population, generated by the genetic algorithm, consists of random individuals. Thus, for example in 6^{th} attempt, the LPC is decreased after 12 generations in contrast to the 4^{th} attempt where the LPC starts to decrease even from the 4^{th} generation.

In general, there are 3 or 4 plateaus for each attempt and the lowest LPC value is reached after steep declines. Because of these steep decreases, the intermediate generations should be examined so that the reasons for these steep changes can be identified.

In order to do that, the analyzer results for the offshore wind farm layouts found in the last attempt of 5^{th} and 6^{th} generations were extracted.

In Table 7-1 all the required data for this comparison are provided.

Table 7-1: Analyzer algorithm results for the 5^{th} and 6^{th} generations during 9^{th} attempt.

Generation	Lowest LPC [€ct/KWh]	Cable length [km]	Cable cost [M€]	Investment cost [M€]	Support structure cost [M€]	Decommissioning cost [M€]	Annual Energy Yield [GWh]
5	9.848	41.808	27.304	424.717	128.24	56.976	683.39
6	9.8241	40.722	26.325	426.075	131.152	57.23	686.45

From the Table above, it can be seen that the annual energy yield is 0.4479% higher in 6^{th} than in 5^{th} generation.

In addition, the Figures below for both generations were retrieved. These Figures illustrate the wind farm layout and the cable topology of these farms.

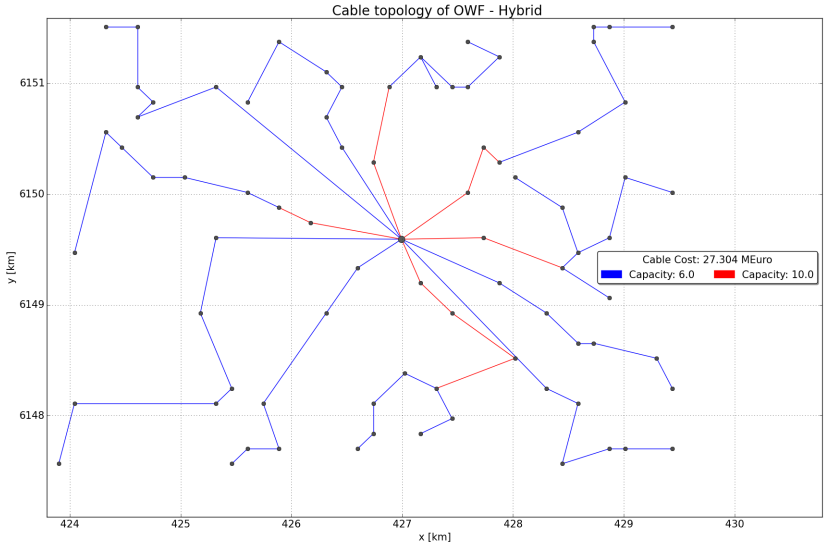

Figure 7-4: Layout and Cable topology of the OWF of 5^{th} generation.

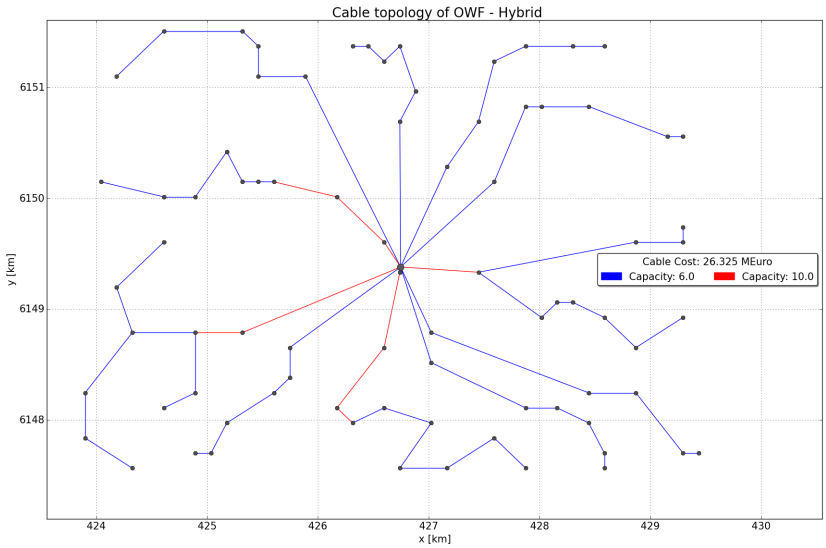

Figure 7-5: Layout and Cable topology of the OWF of 6^{th} generation.

From the Figures and Tables above, it is observed that for both generations there is no great difference between the cable length and between the cable cost. So, the cable topology does not contribute significantly to this steep decrease of the LPC.

In contrast to the cable topology, water depth may have a larger contribution to the steep decrease of the LPC. In Table 7-2, the average water depth values for the layouts of both generations are provided.

Table 7-2: Water depth of each wind turbine for both generations.

Generation	water depth [m]
5^{th} generation	10.436
6^{th} generation	10.063

From that Table, it is concluded that almost all the wind turbines were moved towards shallower waters during the optimization. However, the support structure cost in 6^{th} generation is higher compared to the 5^{th} generation, see subsection 6-3-3. Apart from the total support structure cost, both the total investment cost and the total decommissioning cost of 6^{th} generation are also higher than the corresponding costs of 5^{th} generation. Finally, the annual energy yield is also higher in 6^{th} generation. As a consequence, this will contribute to the reduction of the LPC.

Apart from the above, the analyzer is used for each layout that corresponds to the lowest LPCs (last generation) so as all the required information for each layout to be extracted.

Table 7-3 and Table 7-4 provide all the necessary data for each one of the best layouts found by the GA.

Table 7-3: Analyzer algorithm results for the lowest LPC for each attempt.

Attempt	Lowest LPC [€ct/KWh]	Cable length [km]	Cable cost [M€]	Support structure cost [M€]
1	9.7822	39.834	26.225	129.068
2	9.7794	40.253	26.441	127.048
3	9.8017	39.611	26.03	128.618
4	9.7758	39.986	26.626	128.274
5	9.7907	37.958	25.222	125.187
6	9.7839	41.943	26.943	127.259
7	9.7898	41.538	27.125	126.638
8	9.7797	40.805	26.762	130.782
9	9.7872	41.054	27.093	131.449

Table 7-4: Analyzer algorithm results for the lowest LPC for each attempt.

Attempt	Investment cost [M€]	Decommissioning cost [M€]	Annual Energy Yield [GWh]	Average $O\&M$ cost [M€$/y$]
1	424.298	56.956	687.71	24.888
2	422.8	56.767	686.00	24.851

Attempt	Investment cost [$M€$]	Decommissioning cost [$M€$]	Annual Energy Yield [GWh]	Average $O\&M$ cost [$M€/y$]
3	423.737	56.896	685.65	24.876
4	424.062	56.878	687.72	24.869
5	419.943	56.422	682.58	24.878
6	423.497	56.874	686.68	24.879
7	423.137	56.789	685.94	24.883
8	426.426	57.197	689.92	24.876
9	427.239	57.284	690.20	24.874

From Tables 7-3 and 7-4, it can be observed that after 15 generations the LPC is going to get almost the same value for all the attempts. The average LPC value after 9 attempts is $9.7839€ct/KWh$.

The lowest LPC value was found in 4th attempt, but this value could be even lower if the number of generations was greater. The reason why the genetic algorithm was not tested for a greater number of generations is the high computation time, which is approximately 4 and a half hours.

7-3-3 Scenario 2

The second scenario for the performance of the genetic algorithm is similar to the first one, but now the number of parents is reduced to 10, 20% of the population. Selecting only a few individuals, the algorithm will quickly converge to a specific region without a wider exploration of the solution space. Thus, there is the danger of falling in a local optimum.

The number of generations remained the same so that the results could be comparable to the first scenario.

As far as the number of the attempts is concerned, only four times the genetic algorithm has been tested, due to the high computation time. The average computation time of all the attempts is 27372.531 seconds or 7 hours and 36 minutes. The increase in computation time compared to the first scenario is due to the low number of parents. In this case, the genetic algorithm needs more time to give birth to the new individuals.

Similarly to the first scenario, the number of generations is 15 and the GA tries to find a lower LPC than the previous generation. The following graphs illustrate how the LPC is changed in relation to the generations for the 4 attempts of the genetic algorithm.

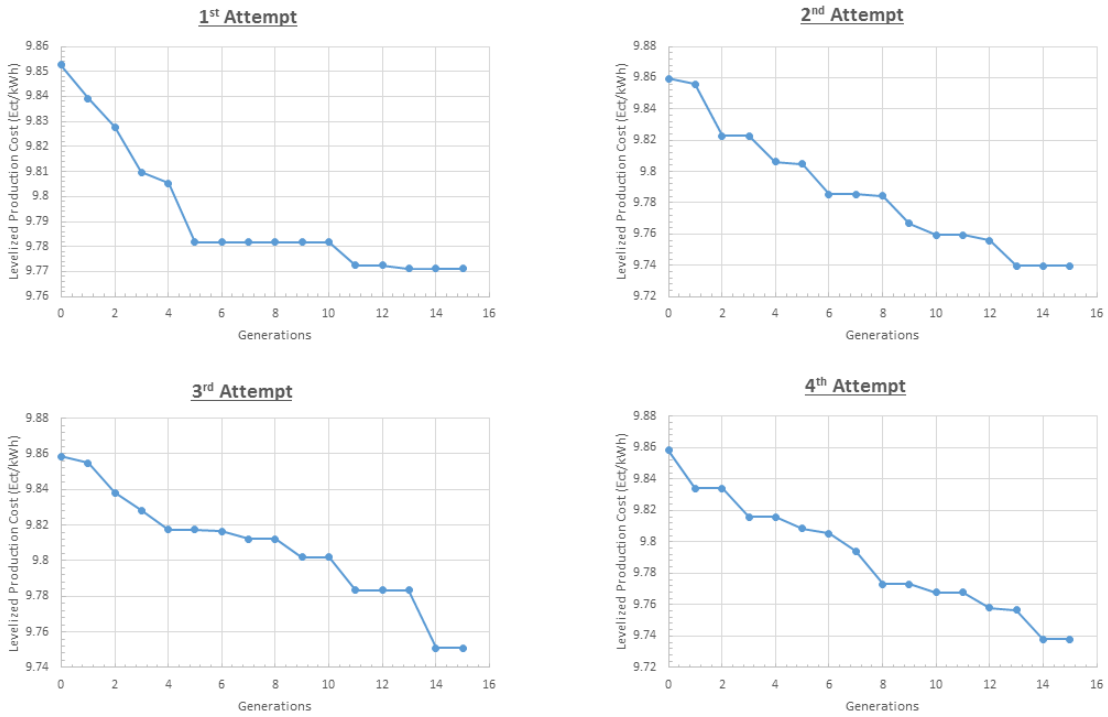

Figure 7-6: Levelized Production Cost [€ct/KWh] versus number of generations for the second scenario.

From Figure 7-6, it is noticed that again the lowest LPC value is achieved in the last generations of each attempt.

In contrast to the first scenario, the LPC reduction is smoother, apart from very few instances where the LPC decrease is steeper. The reason for these steep declines is again the position change of the already shallow wind turbines to even shallower waters and the difference in investments and decommissioning costs.

Once again, the LPC is going to take almost the same value after a certain number of generations for all the attempts. The average value of the levelized production cost for this scenario is 9.745€ct/KWh.

Tables 7-5 and 7-6 provide the most important information for the final LPC of each attempt, by using the analyzer.

Table 7-5: Analyzer algorithm results for the lowest LPC for each attempt.

Attempt	Lowest LPC [€ct/KWh]	Cable length [km]	Cable cost [M€]	Support structure cost [M€]
1	9.7711	38.36	25.046	127.492
2	9.7395	38.556	25.935	126.937

Attempt	Lowest LPC [€ct/KWh]	Cable length [km]	Cable cost [M€]	Support structure cost [M€]
3	9.7508	39.944	26.778	128.785
4	9.7379	41.309	27.446	129.585

Table 7-6: Analyzer algorithm results for the lowest LPC for each attempt.

Attempt	Investment cost [M€]	Decommissioning cost [M€]	Annual Energy Yield [GWh]	Average $O\&M$ cost [M€/y]
1	421.804	56.699	685.95	24.887
2	422.282	56.654	688.57	24.880
3	424.753	56.938	690.02	24.854
4	426.064	57.091	691.95	24.823

Comparing both scenarios, it can be observed that when fewer parents are used, then better OWF layouts can be found, in terms of lower LPC values. More specifically, in scenario 1 the lowest LPC value was equal to 9.7758€ct/KWh while in the second scenario was equal to 9.7379. In addition, the annual energy yield is higher in 2^{nd} scenario than in the 1^{st} one.

7-3-4 Scenario 3

In the third scenario, 30 parents were used again, but the number of the wind turbines was decreased to 30 turbines. Moreover, the number of generations was increased from 15 to 20, since the computation time is lower by using lower number of wind turbines. In that case, it can be in more depth investigated if the LPC can take even lower values. The number of population remained the same as before.

The average computation time for the current scenario was 3376.354 seconds or 56 minutes.

As far as the number of the attempts is concerned, the genetic algorithm was tested 5 times for this scenario. It could be tested for more than five times, since the computation time is relatively low, but 5 times are enough to examine the performance of the optimization tool.

Using the genetic algorithm under these conditions, Figure 7-7 was obtained. The following graphs illustrate how the LPC values change in relation to the generations for the third scenario.

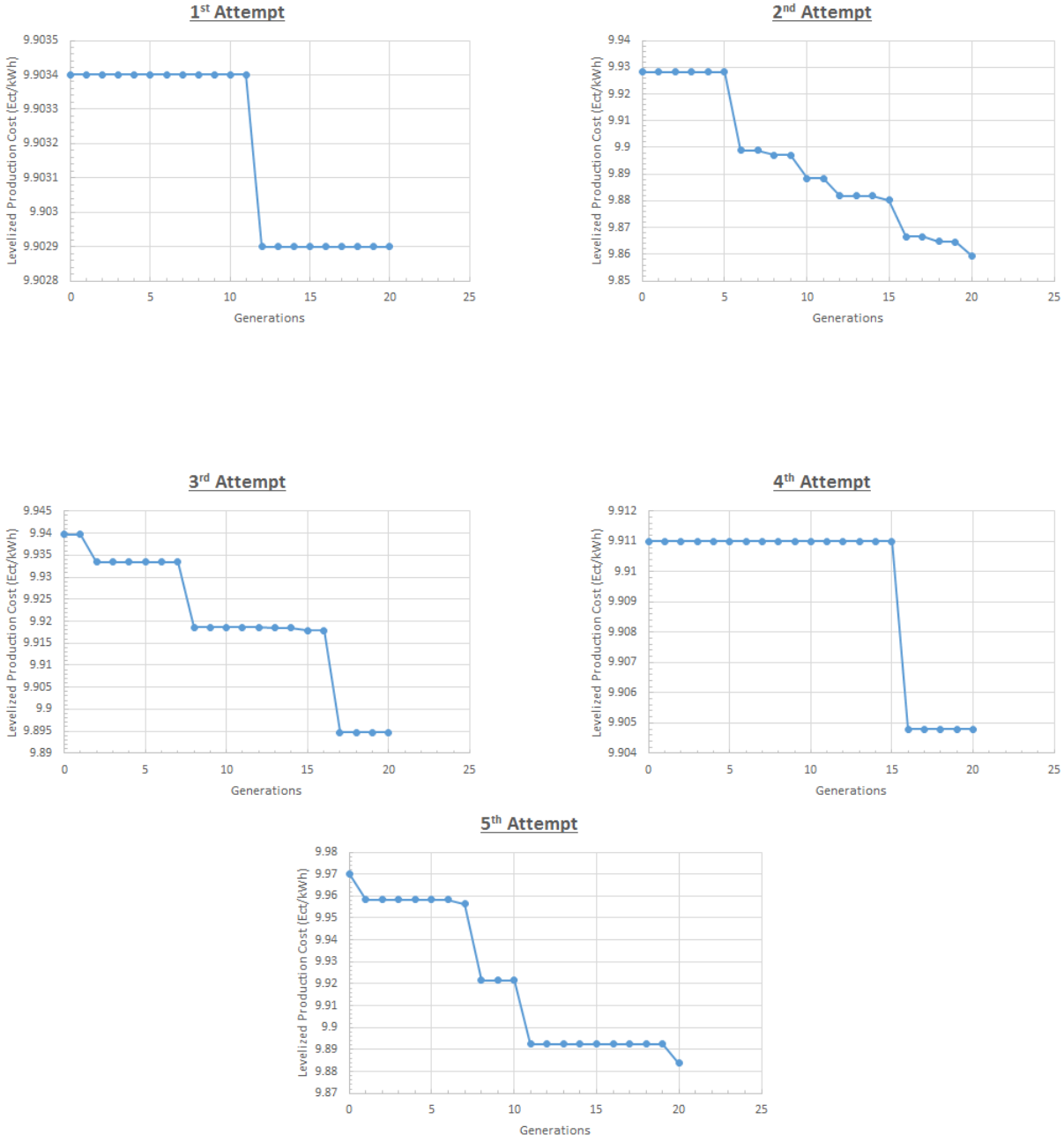

Figure 7-7: Levelized Production Cost [€ct/KWh] versus number of generations for the third scenario.

From Figure 7-7, it is shown that after 15 generations, the LPC is going to take almost the same value for all the attempts. In addition, a similarity with the first scenario is that there are frequent steep decreases of the LPC values. This may occurs, because of the parents number. In both scenarios 30 parents were used.

As it can be seen from the Figure above, the last generation has the best results, as it was expected. The analyzer results for these layouts are summarized in the following Tables.

Table 7-7: Analyzer algorithm results for the lowest LPC for each attempt.

Attempt	Lowest LPC [€ct/KWh]	Cable length [km]	Cable cost [M€]	Support structure cost [M€]
1	9.9029	19.295	12.254	46.151
2	9.8594	17.374	11.155	45.999
3	9.8947	18.239	11.814	45.909
4	9.9048	17.87	11.523	46.575
5	9.8837	17.677	11.365	45.884

Table 7-8: Analyzer algorithm results for the lowest LPC for each attempt.

Attempt	Investment cost [M€]	Decommissioning cost [M€]	Annual Energy Yield [GWh]	Average $O\&M$ cost [M€$/y$]
1	169.625	23.599	273.26	10.097
2	168.343	23.474	273.00	10.079
3	169.121	23.513	273.02	10.101
4	169.182	23.565	272.75	10.095
5	168.522	23.478	272.74	10.102

By using 30 wind turbines, the lowest value of the levelized production cost is 9.8594€ct/KWh and the corresponding annual energy yield is equal to 273GWh.

Furthermore, it would be of great importance to be presented, how the layouts of the offshore wind farm has changed using only 30 wind turbines. This will be done for the layout of the 2^{nd} attempt, which is the best one. It is also interesting to be mentioned that the second attempt has the lowest LPC, not because of high annual energy yield, but due to the fact that all the costs are lower than the other attempts. Only the support structure costs are not the lowest, but they are not too high compared to the other attempts.

Figure 7-8 illustrates both the layout and the cable topology of the offshore wind farm.

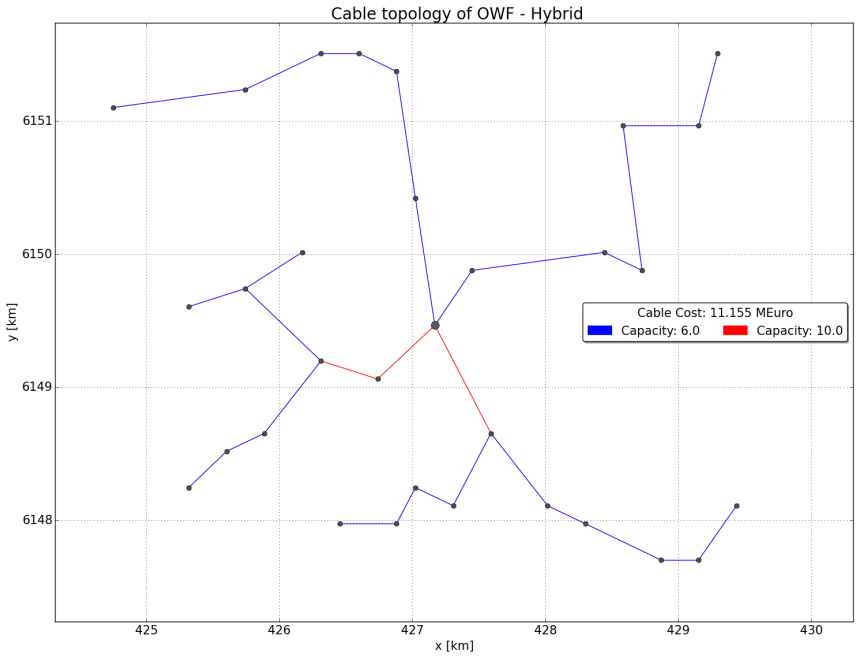

Figure 7-8: Layout and cable topology for the OWF with the lowest LPC of third scenario.

From the Figure above, it can be noted that the majority of the wind turbines are placed to shallow waters (left side of the Figure).

7-3-5 Scenario 4

In the last scenario, all the parameters remained the same apart from the number of parents, which reduced to 10. The number of generations remained the same, since 30 wind turbines were used.

For this last scenario the computation time, required by the optimization tool, was 5834.013 seconds or approximately 1 hour and 37 minutes. This increase in computation time is caused by the low number of parents. In that case, the genetic algorithm needs more time to give birth to the new children/individuals.

As in previous scenarios, using the GA Figure 7-9 was obtained.

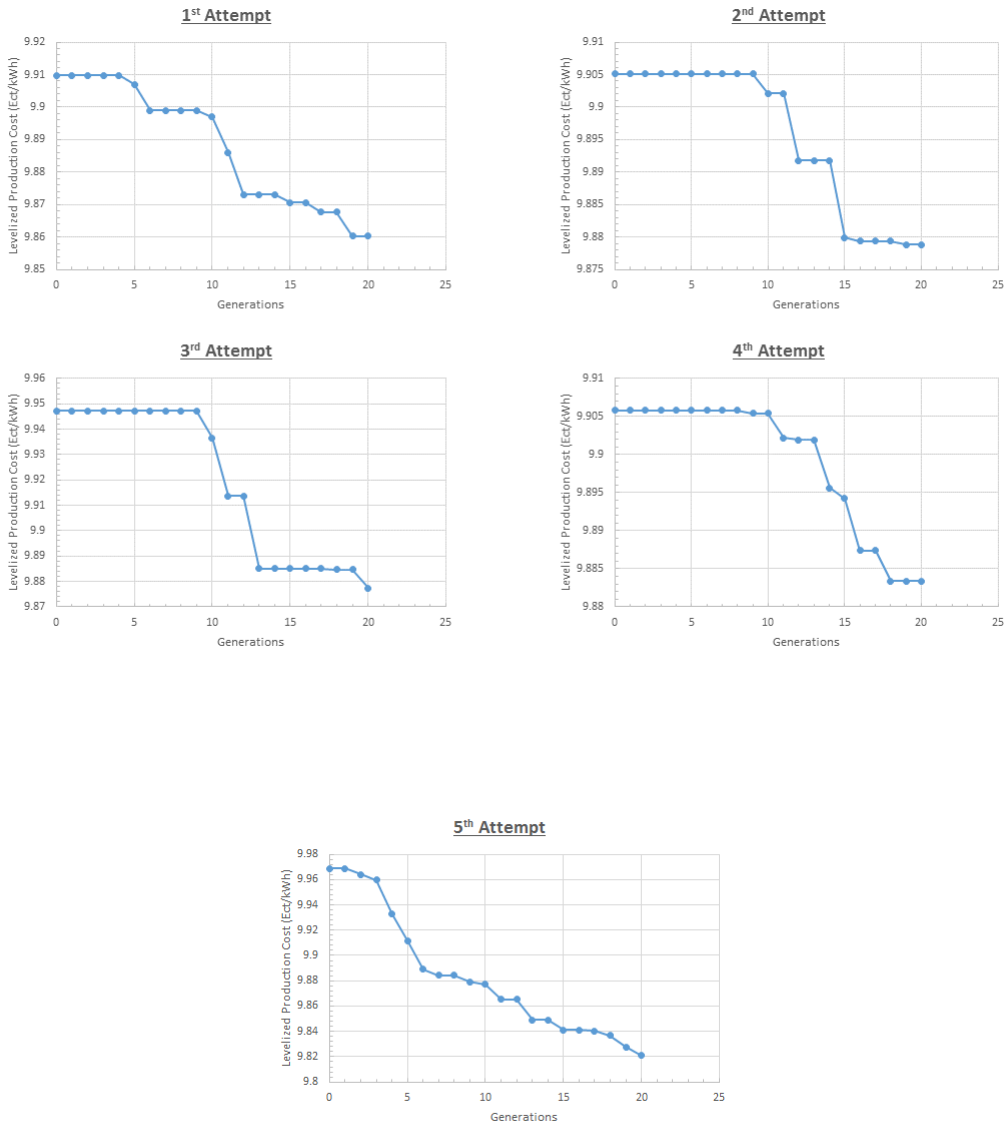

Figure 7-9: Levelized Production Cost [€ct/KWh] versus number of generations for the fourth scenario.

Similarly to the other 3 scenarios, the LPC converges to an almost same value after 20 generations. For the current scenario, the average value of the best LPCs is equal to 9.8773€ct/KWh.

It can be observed, that there are some steep decreases of the LPC, but they are smoother compared to the previous scenario, where 30 parents were used.

In addition, for each one of the lowest LPCs the analyzer results were extracted.

Table 7-9: Analyzer algorithm results for the lowest LPC for each attempt.

Attempt	Lowest LPC [€ct/KWh]	Cable length [km]	Cable cost [M€]	Support structure cost [M€]
1	9.8603	17.461	11.105	45.667
2	9.8788	17.631	11.369	46.396
3	9.8773	16.411	10.558	45.2
4	9.8834	17.191	11.156	45.032
5	9.8211	15.656	10.173	45.199

Table 7-10: Analyzer algorithm results for the lowest LPC for each attempt.

Attempt	Investment cost [M€]	Decommissioning cost [M€]	Annual Energy Yield [GWh]	Average $O\&M$ cost [M€$/y$]
1	168.192	23.441	273.13	10.109
2	168.939	23.531	273.37	10.109
3	167.187	23.329	271.81	10.126
4	167.706	23.357	271.89	10.099
5	166.705	23.286	272.58	10.096

From Tables 7-9 and 7-10, it can be noted that the best layout has an LPC equal to 9.8211€ct/KWh and annual energy yield equal to approximately 273GWh. Furthermore, the low value of the LPC is due to a combination of high energy yield and low investment, decommissioning and cable costs.

7-3-6 Discussion

In general, it should be mentioned that the genetic algorithm developed in the current MSc Thesis works properly, since it is always able to find a better solution. More specifically, the GA finds in each generation a lower LPC or retains the same LPC value if it cannot to find a lower one.

In addition, the GA is equally well-performed, either when 80 wind turbines or 30 wind turbines are used. That means that the user can implement the developed optimization tool for various number of wind turbines. The most important difference between a small and a large number of turbines is that in the first case the computation time is significantly lower than in the second one. The computation time is a very important parameter and in most of the cases the main parameter for the optimization tools. Furthermore, using a smaller number of turbines the LPC values are higher compared to the corresponding values when a larger number of turbines is used.

Last but not least, the number of selected parents influence the results. The use of a lower number of parents will give better solutions, but the GA needs more time to find the best

solution for the same number of generations. However, it is not that high to influence the user's option. This argument can be more clear observing Figure 7-10, in which the layouts with the lowest LPCs from the last two scenarios are compared. So, it can be noted that using a lower number of parents (red line) most of the LPC values are lower compared to a higher parent number (blue line) for the same number of generations.

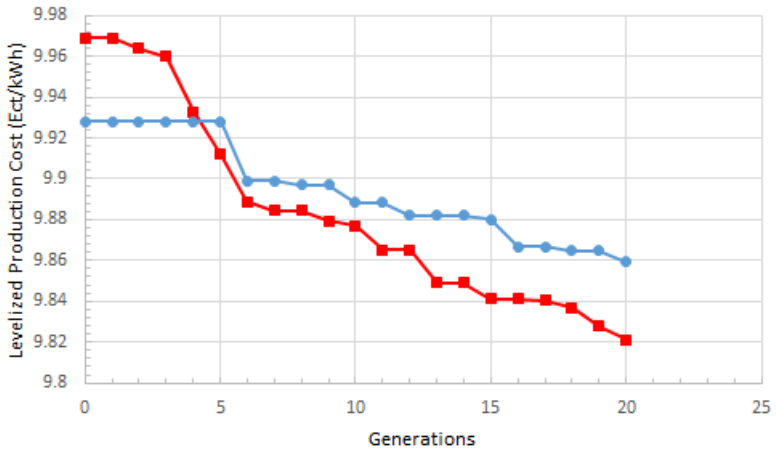

Figure 7-10: Levelized Production Cost [€ct/KWh] versus number of generations for 3^{rd} (blue line) and 4^{th} (red line) scenarios.

Chapter 8

Case Studies

This chapter provides the different case studies that were examined in the current work, using the developed optimization tool, described in chapter 7. These case studies are not related to the parameters of the Genetic Algorithm (GA) as in previous chapter, but they focus mostly on changes inside the analyzer. The purpose of these case studies is to assess how each of the analyzer ingredients affect the layout optimization.

8-1 Introduction to the Case Studies

Taking into consideration the comparison between the four scenarios and the discussion of subsection 7-3-6, the following case studies will be implemented using 10 parents and 20 generations, since in that case the optimization tool performs better. Moreover, 30 wind turbines will be used because the lower the number of the wind turbines is the lower the computation time is as well. The number of population will remain the same as in the 4 scenarios, namely 50.

In addition, it must be mentioned that the same seabed shape will be used for all the case studies. More specifically, the seabed consists of 3 linear surface planes, 2 linearly sloped and one flat surface plane between the two sloped ones, see Figure 8-1. In order to define these surface planes, it was assumed that 9 points inside the wind farm are known, which means that the x, y and z coordinates for these points are known. Each surface plane uses 3 points so as to be defined and they were be chosen randomly.

Figure 8-1 illustrates the aforementioned seabed.

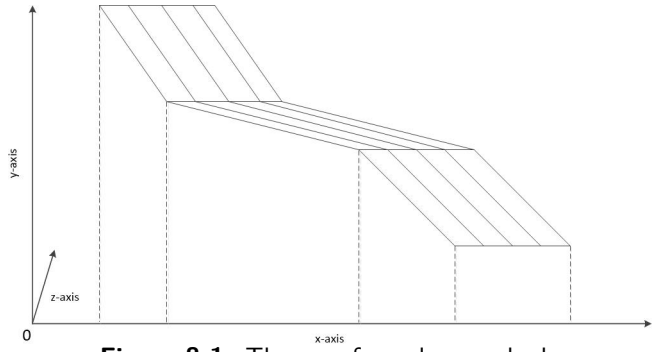

Figure 8-1: Three surface plane seabed.

Furthermore, each case study was tested more than one time. Specifically, the optimization tool was realized more than one time for each case so that the results will be validated.

For the current work four case studies were examined:

- Use of a three surface plane seabed. It is expected that this case study will provide the best solution for the Levelized Production Cost (LPC) compared to the next case studies, since all the three ingredients in the analyzer contribute to the layout optimization of the Offshore Wind Farms (OWF). The comparison among the case studies will be given after the results presentation for all the case studies.
- Use of the same support structure design in each individual. It is expected that the the support structure cost will be increased compared to the first case study since wind turbines in each individual will use the same support structure design, which will be the most expensive one.
- Use of the same support structure design for all individuals. In this case study, it is expected that the support structure cost will be even higher compared to the first two case studies since all the wind turbines in all individuals will have the same support structure design. This support design will be the most expensive in the whole wind farm area.
- Use of constant infield cable cost. Here, it is expected that the support structure cost will be more or less the same with the one of the first case study since each wind turbine has its own support structure design. However, the investment cost is expected to be increased because of using constant cable cost.

In the following sections the 4 case studies and their corresponding results are presented.

8-2 Case Study 1: Use of a three surface plane seabed

In the first case study, all the ingredients in the analyzer will remain as they are, but the seabed shape will be the one described in section 8-1. Thus, all the three elements will contribute to the optimization of the OWF layout.

For this case study the optimization tool was tested five times so that the results will be validated.

The analyzer results for the best layout of each attempt are presented in Tables 8-1 and 8-2.

Table 8-1: Analyzer algorithm results for the lowest LPC for each attempt.

Attempt	Lowest LPC [€ct/KWh]	Cable length [km]	Cable cost [M€]	Support structure cost [M€]
1	9.8691	18.103	11.608	45.973
2	9.8119	15.983	10.621	46.44
3	9.8437	16.278	10.326	46.086
4	9.8871	17.202	10.93	46.478
5	9.8694	16.405	10.439	45.957

Table 8-2: Analyzer algorithm results for the lowest LPC for each attempt.

Attempt	Investment cost [M€]	Decommissioning cost [M€]	Annual Energy Yield [GWh]	Average $O\&M$ cost [M€$/y$]
1	167.89	23.515	272.78	10.127
2	167.304	23.445	273.55	10.105
3	166.675	23.424	272.21	10.121
4	167.658	23.518	272.17	10.138
5	166.673	23.416	271.75	10.146

From these two Tables, it can be noted that the second attempt is the best solution when all the ingredients inside the analyzer participate in the optimization. The most important information is the cable cost, the support structure cost and the annual energy yield, because they have large contribution to the optimization.

In Figure 8-2 the cable topology and the layout of the farm with the lowest LPC are depicted.

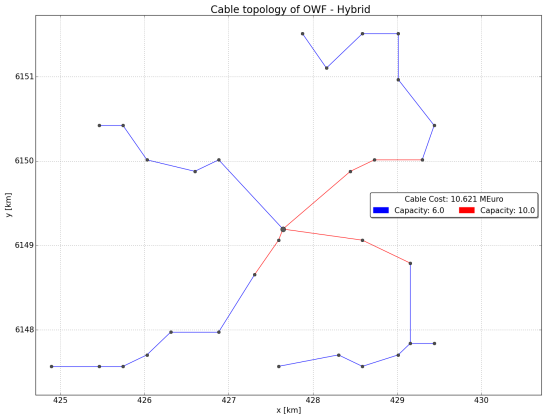

Figure 8-2: Layout and cable topology for the OWF with the lowest LPC.

8-3 Case Study 2: Use of the same support structure design in each individual

In the second case study, all the wind turbines in each individual will have the same design for the monopile support structure. Thus, there will be not support structure variation in this case study and only the other two ingredients in the analyzer, namely Jensen algorithm and Hybrid algorithm will contribute to the optimization.

In order to have the same design for all the support structures, the piles must be designed in such a way that they all will able to withstand extremes of wind speed and storm waves. One could say that using the support structure design of the deepest turbine for all the wind turbines then all the piles could be built properly. However, this is not the case as it was described in subsection 6-3-3. So, taking into consideration the aforementioned subsection, all the support structures will be designed based on the most expensive support structure in each individual. Thus, an individual with no turbines in shallow water will have a support structure design that is suitable for deeper waters.

More specifically, the optimizer will calculate the most expensive support structure in each individual and then it will use this pile design for all the wind turbines. The total support structure cost can be found by multiplying the aforementioned cost with the number of the wind turbines in this individual.

The optimization tool was tested three times for this case study.

Similarly to the first case study, the analyzer results for the best layout of each attempt are presented in Table 8-3 and Table 8-4.

Table 8-3: Analyzer algorithm results for the lowest LPC for each attempt.

Attempt	Lowest LPC [€ct/KWh]	Cable length [km]	Cable cost [M€]	Support structure cost [M€]
1	10.481	16.654	10.804	50.869
2	10.4226	17.738	11.18	51.751
3	10.5081	16.731	10.868	52.884

Table 8-4: Analyzer algorithm results for the lowest LPC for each attempt.

Attempt	Investment cost [M€]	Decommissioning cost [M€]	Annual Energy Yield [GWh]	Average $O\&M$ cost [M€/y]
1	171.558	23.98	270.83	11.226
2	172.758	24.137	273.56	11.233
3	173.476	24.208	271.61	11.19

In addition, Table 8-5 provides the water depth of each attempt where the support structure is the most expensive. More specifically, these water depths are the shallowest water depths at which a turbine can be found in the optimized individual.

Table 8-5: Water depth for the most expensive support structure.

Attempt	Water depth [m]
1	8.331
2	8.179
3	7.995

As it was expected, the most expensive support structures are in shallower waters, (see subsection 6-3-3). Furthermore, the wind turbines have been moved towards deeper waters during the optimization, since now the most expensive support structures are not in the shallowest water depth of the wind farm area (approximately 6 meters) but in a water depth of approximately 8 meters, see Table 8-5.

From Tables 8-3 and 8-4, it can be noted that the support structure costs are higher compared to the ones of the first case study. This is an expectable difference, since in the current case study all wind turbines has the same support structure which is the most expensive at the same time.

This increase in the support structure costs will also cause an increase in the investment, $O\&M$ and decommissioning costs.

As far as the cable cost and cable length are concerned, there are not big differences between the first and the second case study, since the Hybrid algorithm is kept the same in both

cases. More specifically, the average value of the cable cost and cable length is $10.868 M€$and $16.731 km$ respectively. For the first case study the corresponding values are $10.621 M€$and $16.405 km$.

Finally, the annual energy yield is also almost the same for both cases, since no changes were done in the algorithm for the wake effects.

Thus, due to all the above, it makes sense the fact that the LPC is larger in the current case study.

8-4 Case Study 3: Use of the same support structure design for all individuals

This case study is similar to the previous one but now all the wind turbines will have the same support structure design for all individuals. For that case the most expensive support structure within the whole wind farm area is selected.

As it has already be seen in subsection 6-3-3, the most expensive support structure is found in the shallowest water depth of the farm, approximately 6 meters. For that reason, the design of the support structure placed in the shallowest water depth will be used for all the wind turbines. The total support structure cost of the farm can be found by multiplying the cost of the most expensive support structure with the total number of the wind turbines in the wind farm.

Similarly to the previous case study, the optimization tool was tested three times.

In addition, the analyzer results for the best layouts of each attempt are presented in Tables 8-6 and 8-7.

Table 8-6: Analyzer algorithm results for the lowest LPC for each attempt.

Attempt	Lowest LPC [€ct/KWh]	Cable length [km]	Cable cost [M€]	Support structure cost [M€]
1	11.3168	18.695	11.937	73.709
2	11.3274	18.971	12.448	73.709
3	11.3023	17.656	11.376	73.709

Table 8-7: Analyzer algorithm results for the lowest LPC for each attempt.

Attempt	Investment cost [M€]	Decommissioning cost [M€]	Annual Energy Yield [GWh]	Average $O\&M$ cost [M€$/y$]
1	193.808	26.538	274.64	11.708
2	194.334	26.553	274.79	11.702
3	193.231	26.479	274.43	11.702

From Tables 8-6 and 8-7, it can be seen that the support structure costs are higher compared to the second case study. This increase was expected, since in the current case study the most expensive support structure of the whole wind farm is used for all the wind turbines. In contrast, in the second case each individual has its own most expensive support structure which is not mandatory in the shallowest area of the wind farm.

This increase will also cause an increase to the investment, $O\&M$ and decommissioning costs. In addition, taking into account that the average value of annual energy yield is almost the same in both cases then it is reasonable that the LPCs are also higher. Regarding the cable cost and cable length, there are not big differences since the Hybrid algorithm is used in both cases without changes.

8-5 Case Study 4: Use of constant infield cable cost

In the fourth case study, the infield cable cost will be kept the same for all the individuals/layouts.

More specifically, the analyzer uses the cost model of the Hybrid algorithm for the calculation of the cable cost. However, the optimizer uses this cost model only for the cable cost calculation of the initial population. Afterwards, the average cable cost value of the initial population is calculated and it is used as a fixed value for every individual and for all generations.

Thus, the Hybrid algorithm is "switched-off" for the current case study and only the other two ingredients of the analyzer, namely wake effect algorithm and support structure variation, will contribute to the layout optimization.

The optimization was also tested tree times under these changes. In addition, the analyzer results are presented in

The analyzer results for the best layout of each attempt are presented in Table 8-8 and Table 8-9.

Table 8-8: Analyzer algorithm results for the lowest LPC for each attempt.

Attempt	Lowest LPC [€ct/KWh]	Cable length [km]	Cable cost [M€]	Support structure cost [M€]
1	9.9051	22.9	13.276	47.3
2	9.9295	21.036	13.199	47.749
3	9.8879	22.673	13.160	47.08

Table 8-9: Analyzer algorithm results for the lowest LPC for each attempt.

Attempt	Investment cost $[M€]$	Decommissioning cost $[M€]$	Annual Energy Yield $[GWh]$	Average $O\&M$ cost $[M€/y]$
1	170.829	23.933	274.77	10.128
2	171.162	23.878	274.66	10.153
3	170.506	23.897	274.99	10.135

From Table 8-8, it can be seen that the LPC values are slightly higher compared to the first case study where the Hybrid algorithm was not "switched-off". This outcome was expectable, since in the current case the optimizer uses a fixed value for the cable cost and there is no possibility for the optimizer to find a better solution. Thus, the investment costs, the $O\&M$ costs and the decommissioning costs will be increased.

8-6 Discussion

In general, it should be mentioned that all the three ingredients inside the analyzer affect the layout optimization of an OWF. The wake effect algorithm has not been changed during the case studies because wake effects play the most dominant role in the layout optimization and they must always be taken into consideration.

The results of the 4 case studies have been compared. Specifically, comparing the best layouts of the different case studies the following graph was found.

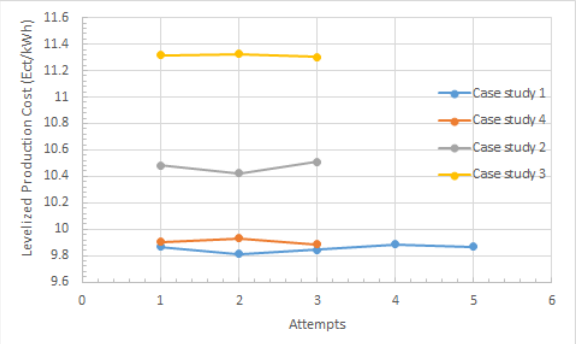

Figure 8-3: Levelized Production Cost $[€ct/KWh]$ versus number of attempts.

From this graph it can be observed that by "switching-off" either the support structure variation or the Hybrid algorithm then the layout optimization will be affected. Taking as reference the first case study, it is clear that the support structure variation has a larger contribution to the layout optimization than the cables. As it can be seen from the graph, the LPC values of the second and third case have been increased significantly compared to the ones of third case.

The main reason for this difference is the support structure cost. Both in the second and third case study the support structure cost is increased significantly since the most expensive support structure design is used in each individual and in the whole farm respectively. This increase causes an increase to investment, $O\&M$ and decommissioning costs as well. As a consequence the LPC values are higher for these two cases compared to the other two cases, where each wind turbine has its own support structure design. For the latter case studies, the optimizer move the wind turbines to deeper water depths where the support structure is cheaper, see subsection 6-3-3.

Regarding the computation time, the following graph is obtained.

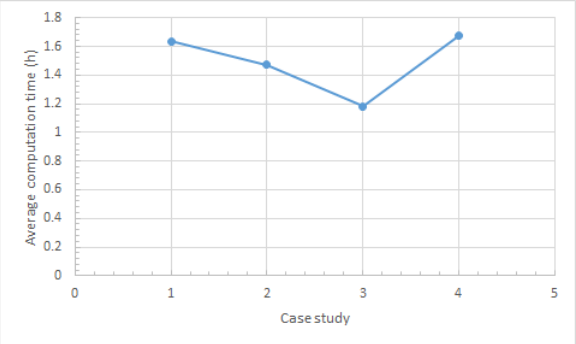

Figure 8-4: Levelized Production Cost [€ct/KWh] versus number of attempts.

From Figure 8-4 it can be seen that the first and the last case study demand more computation time than the other two cases. This is reasonable because in these case studies each wind turbine has its own support structure design. This means that the analyzer needs more time to calculate all the different designs and costs compared to the second and third cases, where the same support structure design is used for all wind turbines in each individual and whole farm respectively.

Chapter 9

Conclusions and Recommendations

The final chapter provides the main conclusions and recommendations regarding future work.

9-1 Conclusions

The primary objective of the thesis was to determine the importance of each of the three ingredients, namely wake effects, cable topology and support structure variation, for the layout optimization. For that purpose, a tool for the optimization of Offshore Wind Farms (OWF) combining these three elements has been developed. The key objective throughout the optimization was chosen to be the cost minimization.

The first sub−goal of the current project was to find a way to implement the aforementioned ingredients. In order to do that tools/algorithms from previous projects have been used. More specifically, Jensen wake model, developed by [4], was used, while the Hybrid approach, developed by [2] was implemented for the cable topology. Regarding the support structure variation, part of the MZ tool[1] was used.

Subsequently, after the necessary changes and additions in the aforementioned algorithms, the three elements have been combined in one algorithm, called analyzer. For the performance of the analyzer, the layout of the Horns Rev 1 Offshore Wind Farm (OWF) was used as a case study. The purpose of that case study was to prepare the 3 analyzer ingredients and test their suitability for the optimization tool. The final output of the analyzer was the Levelized Production Cost (LPC), which is influenced from all the three analyzer ingredients. As far as the wake algorithm is concerned, different wind direction bin sizes were used so that the most suitable one could be selected. More specifically, the wind direction bin of 8 degrees was the most suitable in terms both of Levelized Production Cost (LPC) value and computation time, since the LPC value was almost the same with the one of the 1-degree wind direction bin (high accuracy) and the computation time was much smaller compared again to the 1-degree wind direction bin. Regarding the cable topology, Hybrid algorithm found to be suitable for the purpose of the current project, since it is highly sensitive and it always tries to find the most cost effective cable topology. Specifically, it was found that even small changes in

position of one wind turbine inside the farm caused changes in cable topology. This behavior was observed for wind turbines both close to substation and far from it. Finally, the use of the MZ tool was found to be inconclusive. On one hand, it was suitable for the calculation of different support structure designs, since it was found that the support structure variation influences the support structure cost and as a result the final total cost of the farm. On the other hand, the support structure variation does not depend only on the water depth, but wave height affected a lot the support structure design and the corresponding cost. In particular, using higher wave height value, the support structure cost was smaller in deeper water. That behavior was not expected in the first place and further research on the wave height part should be done in the future.

Furthermore, another sub−goal of the project was to find a way to realize optimization by simultaneously considering these three ingredients. That has been done by developing an optimization tool based on the genetic algorithm logic. The fitness/objective function of the optimizer was the Levelized Production Cost, which was calculated by the analyzer. In order to test the performance of the optimization tool four different scenarios were examined. These scenarios were related to the values of some of the optimization tool parameters such as the number of parents, the number of generations and the number of the wind turbines. After the implementation of the optimization tool, it was found that the optimizer works properly and it was able to find a better solution in terms of a lower LPC value. However, it was difficult to observe when the LPC value converges, since the way that the LPC is reduced is not gradual. Another remark on the convergence is that the LPC may take even lower values, but then the optimizer will need more computation time because the number of generations will be higher. So there is a tradeoff between the LPC values and the computation time.

In addition, the current optimization tool can be used both for small and for large offshore wind farms, since it was found that it works equally properly, either when 80 wind turbines or 30 wind turbines were used. Finally, it must be noted that the number of parents played an important role to the final results, since the lower this number was the better the results were, namely lower the LPC values were.

Moreover, in order to assess how each of the analyzer elements affect the layout optimization, four case studies were examined. These case studies were related to changes in the algorithms of the 3 analyzer ingredients. Apart from the changes in the analyzer, the seabed shape has been also changed for the same purpose. After the implementation of the optimization tool for all the case studies, it was found that all the three ingredients namely wake effects, cable topology and support structure variation affect the layout optimization of an OWF. Furthermore, a conclusion of great importance is that the support structure variation had the largest contribution to the layout optimization than the cable topology. Support structure variation caused large increase to the support structure cost and as a consequence to the total cost. More specifically, for the cases that the wind turbines used the same support structure design in each individual and in all individuals, the average LPC value increased 6% and 14% respectively compared to the reference case, where all the ingredients contribute to the optimization. Finally, for the case of constant cable cost the LPC value increased only 0.5% compared to the reference case.

As far as the computation time is concerned, it was concluded that in case that each wind turbine had its own support structure design the average computation time was higher. More specifically, the computation time was 11%-41% higher when each wind turbine had its own

support structure design. This range in computation time occurred due to different case studies. The higher computation time occurred because the analyzer needed more time for the calculation of all costs.

9-2 Recommendations and Future work

During the development of the program, it is assumed that the $O\&M$ costs are equal to 6% of the total investment costs. It is recommended to be found a more detailed cost model for the $O\&M$ costs that will calculates all the relevant costs that take part in the $O\&M$ costs, such as the costs for the required repairs, the vessels access, the personnel, the subsea inspection and etc. In that way, the $O\&M$ costs will be closer to reality and this will also affect the LPC value.

Furthermore, it is recommendable to be developed a model that will adjust the wave height according to the water depth. The support structure design depends not only on the water depth but also on the wave height. As it was found in the current work, the wave height plays a very important role to the support structure design and it is recommendable not to use a single wave height value for the whole wind farm area, but multiple values according to the environmental conditions.

The computation time can be affected by the selection of certain parameters both in the analyzer and in the optimizer. In the analyzer, some of these parameters are the wind direction bin sizes, the number of wind rose sectors and the selection of wake model.

For the optimizer, the number of parents, the number of individuals, the number of generations and the number of the wind turbines contribute significantly to the computation time. It is then recommended for the user to try different values for these parameters in order to understand how they affect the computation time. In addition, it is recommended for the user to implement different wind and site conditions so as to verify how sensitive the tool output is to these conditions.

Regarding the shape of the seabed, it is recommended to be used more complex shapes in order to be closer to real cases. Finally, a soil variation (sandy, clay, rocky soils) could be used in a future work, since this could play important role to the foundation costs.

Appendix A

The Hybrid algorithm

In Appendix A the detailed structure of the Hybrid approach for the infield cable topology optimization, used in the current Thesis, is provided. Both inputs and outputs are also provided. Finally, the RouteOpt algorithm is presented.

A-1 Inputs and Outputs

Inputs

Turbines: $T = t_1, ..., t_T, t_i = (x_i, y_i)$
Substations: $S = s_1..., s_S, s_i = (x_i, y_i)$
Infield Cables: $R = r_1, ...r_R, r_i = (n_i, c_i)$
Transmission Lines: $((s_{x_0}, s_{y_0}, (s_{x_1}, s_{y_1}))\forall s \in S$
Pipelines/Cables: $((\alpha_{x_0}, \alpha_{y_0}), (\alpha_{x_1}, \alpha_{y_1})$
Crossing penalty: p
Switchgear: $sw = 2$ or 3

Outputs

Connections: $P = (u_{k_1}, u_{v_1}, r_i^{k_v})_1, ..., (u_{k_p}, u_{v_p}, r_i^{k_v})_p$
Cable Length: $L = l_1, ..., l_R$
Cable Cost: C
Number of crossings: N

A-2 Hybrid code

1 foreach $i \in T$ **do** $s_i = argmin_{s \in S}\{d(i,s)\}$
2 $P \leftarrow \bigcup_{i \in T} (i, s_i, r_1)$
3 foreach k,$u \in T$, *if* $s_k \equiv s_u$ **do** $sv_{ku} = (d(k,s_k) - d(k,u)) * c_1 + (N_{ks_k} - N_{ku}) * p$
4 $SV_1, SV_2 \leftarrow$ sorting of $sv_{ku} > 0$ according to decreasing saving
5 repeat
6 *(k,u)* $\leftarrow$ *next element in* SV_1
7 *turbines* $\leftarrow$ *the total number of turbines in the routes containing k and u*
8 **if** *k and u are in different routes* **and** $(k, s_k) \in P$ **and** *u has only one neighbour in P,*
9 **and** *turbines* $\leq n_1$,
10 **and** *(k,u) does not cross any connection in P and transmission line* **then**
11 $P \leftarrow P \setminus ((k, s_k, r_1) \cup (k, u, r_1))$
12 until *end of* SV_1 *is reached*
13 repeat
14 *(k,u)* $\leftarrow$ *maximum saving* sv_{ku} *in* SV_2
15 *turbines* $\leftarrow$ *the total number of turbines in the routes containing k and u*
16 **if** *k and u are in different routes,*
17 **and** *the number of (t,u) connections in P* **foreach** $t \in T < sw - 1$,
18 **and** *(k,u) does not cross any connection in P and transmission line* **then**
19 $i, j \leftarrow$ last clients in the routes containing k and u respectively
20 **if** *turbines* $\leq n_1$ **then**
21 $P \leftarrow P \setminus ((i, s_i, r_1) \cup (k, u, r_1))$
22 **elif** *turbines* $> n_1$ **then**
23 $n_i \leftarrow$ cable capacity for which $n_{i-1} <$ *turbines* $\leq n_i$
24 $P_{tmp} \leftarrow P \setminus ((i, s_i, r_1) \cup (k, u, r_1))$
25 **upgrade** and **downgrade** connections in P_{tmp} where necessary
26 $sv_{ku} \leftarrow Cost(P) - Cost(P_{tmp}) + (N_{is_i} - N_{ku}) * p$ *and update* SV_2
27 **if** $sv_{ku} = max_{sv \in SV_2}\{sv\}$ **then**
28 $P \leftarrow P_{tmp}$
29 **if** *P was updated* **then**
30 **foreach** *client z of the merged route* **do**
31 **if** $n \in T$ and $sv_{zn} \in SV_2$ **do**
32 $sv_{zn} \leftarrow (d(j,s_j) - d(z,n)) * c_1 + (N_{js_j} - N_{zn}) * p$ *and update* SV_2
33 **delete** sv_{ku} **from** SV_2
34 **elif** *P and* sv_{ku} *were not updated* **then**
35 **delete** sv_{ku} **from** SV_2
36 until $sv_{ku} < 0$
37 $P \leftarrow$ **RouteOpt** (radial parts of the routes for which cable r_1 is used)
38 $L = \{\sum_{(u_k,u_v,r_1^{kv}) \in P} d(u_k,u_v), ..., \sum_{(u_k,u_v,r_R^{kv}) \in P} d(u_k,u_v)\}$
39 $C = \sum_{l_i \in L} l_i * c_i$
40 $N = \sum_{(u_k,u_v,r_i^{kv}) \in P} N_{u_k u_v}$
41 return P, L, C, N

A-3 RouteOpt

RouteOpt (Graph $(T \cup S, P)$, distance $d(k,u)\ \forall\ (k,u) \in P$):

1 foreach *route* $r = i_0 - i_1 - i_2 - ... - i_{l-1} - i_l - ... - i_k$ **do**
2 **repeat**
3 $sv \leftarrow max_{l \in 1,...,k-1}\{d(i_{l-1}, i_l) - d(i_l, i_0)\}$ **if** (i_l, i_0) *does not cross any connection...*
4 *...or transmission line*
5 **if** $sv > 0$ **then**
6 $l \leftarrow$ index for which $d(i_{l-1}, i_l) - d(i_l, i_0) = sv$
7 $P \leftarrow P \setminus ((i_{l-1}, i_l) \cup (i_l, i_0))$
8 $r \leftarrow i_{l-1} - ... - i_2 - i_1 - i_0 - i_l - ... - i_k$
9 **until** *no improvement in r exists*
10 return P

Appendix B

Mathematical expressions of cost models

In Appendix B are presented all the mathematical expressions of cost models that were used for the calculation of both investment and decommissioning costs.

Table B-1: Mathematical expressions of cost models

Cost item	Model
Investment costs	
Management [Euro actual]	$0.03*C_{capital}$
Investment costs - Project development	
Engineering [USD 2003]	$0.037*P_{farm,rated}$
Investment costs - Procurement - Rotor-nacelle	
Purchase [Euro actual]	$C_{RNA}*N_t$
Warranty [Euro actual]	$f_{warranty}*C_{RNA}*N_t$

Cost item	Model
Investment costs - Procurement - Support structure	
Tower [USD 2002]	$2.04*m_{tower}*N_t$
Transition piece [Euro 2007]	$3.75*m_{transition\ piece}*N_t$
Boat landing [USD 2003]	$60{,}000*N_t$
Grout [Euro 2003]	$0.1*m_{grout}*N_t$
Monopile [Euro 2007]	$2.25m_{pile}*N_t$
Scour protection [Euro 2003]	$211*V_{scour\ protection}*N_t$
Investment costs - Procurement - Electrical system	
Transmission cable [Euro 2003]	$50+2.3*(5*m_{copper}+15*m_{insulation})$
Shunt reactor [Euro 2003]	$0.807*(P^{0.7513}_{shunt,onshore}+P^{0.7513}_{shunt,offshore})$
Transformer [Euro 2012]	$(3.06*10^{-3}*P_{turbine,rated}+810)*e^{0.039}*N_t+$ $(1.16*P^{0.7513}_{farm,rated})*(e^{0.039*r_{onshore}}+e^{0.039*r_{offshore}})$
Investment costs - Procurement - Auxiliary	
Measuring tower [Euro 2003]	2,050,000
Onshore premises [Euro 2003]	1,500,000
Offshore platform (Including installation) [SEK 2003]	$\frac{2}{3}*(0.4*10^{-3}*m^2_{jacket}-50*m_{jacket}-80*10^6)$ with: $m_{jacket}=582*d^{0.19}_{water}*(3*10^{-3}*P_{farm,rated}+0.5*10^6)^{0.48}$
Investment costs - Installation	
Foundations [USD 2010]	$1.4*m_{pile}*N_t$

Cost item	Model
Investment costs - Installation - Rotor-nacelle assembly	
Onshore transport [Euro 2001]	$(5.84 * 10^{-3} * D + 0.4) * L + 0.486 * D^{2.64}$
Offshore works [USD 2010]	$3.4 * 10^3 * (h_{hub} + 50) * N_t$
Transmission cable [Euro 2003] [USD 2010]	$500,000(+)178 * l$
Investment costs - Installation - Electrical system	
Dune crossing [Euro 2003]	$1,200,000$
Investment costs - Installation - Auxiliary	
Meteo tower [Euro 2003]	$550,000$
Harbour use [USD 2002]	$0.02 * P_{farm,rated}$
Decommissioning costs	
Management [Euro actual]	$0.03 * C_{decommissioning}$
Decommissioning costs - Removal	
Rotor-nacelle assemblies [Euro actual]	$0.91 * C_{offshore\ works}$
Foundations [Euro actual]	$0.91 * C_{foundation\ installation}$
Transmission cable [USD 2010]	$49 * l$
Offshore platform and meteo tower [USD 2010]	$665,000$
Scour protection [USD 2010]	$33 * V_{scour\ protection} * N_t$

Cost item	Model
Site clearance [USD 2010]	$16,000 * N_t$
Decommissioning costs - Disposal	
Rotor-nacelle assemblies [USD 2010]	$150 * m_{RNA} * N_t$

Appendix C

Horns Rev Original Layout

In Appendix A the original wind turbine positions of the Horns Rev Offshore Wind Farms (OWF) are provided.

Table C-1: Horns Rev Original Layout

Coordinates		
No.	X [m]	Y [m]
1	423974	6151447
2	424033	6150889
3	424092	6150332
4	424151	6149774
5	424210	6149216
6	424268	6148658
7	424327	6148101
8	424386	6147543
9	424534	6151447
10	424593	6150889

Table C-2: Horns Rev Original Layout

Coordinates		
No.	X [m]	Y [m]
11	424652	6150332
12	424711	6149774
13	424770	6149216
14	424829	6148658
15	424888	6148101
16	424947	6147543
17	425094	6151447
18	425153	6150889
19	425212	6150332
20	425271	6149774
21	425330	6149216
22	425389	6148658
23	425448	6148101
24	425507	6147543
25	425654	6151447
26	425713	6150889
27	425772	6150332
28	425831	6149774
29	425890	6149216
30	425950	6148659
31	426009	6148101
32	426068	6147543
33	426214	6151447
34	426273	6150889
35	426332	6150332
36	426392	6149774
37	426451	6149216
38	426510	6148659
39	426569	6148101
40	426628	6147543
41	426774	6151447
42	426833	6150889
43	426892	6150332
44	426952	6149774
45	427011	6149216
46	427070	6148659

Table C-3: Horns Rev Original Layout

Coordinates		
No.	X [m]	Y [m]
47	427129	6148101
48	427189	6147543
49	427334	6151447
50	427393	6150889
51	427453	6150332
52	427512	6149774
53	427571	6149216
54	427631	6148659
55	427690	6148101
56	427749	6147543
57	427894	6151447
58	427953	6150889
59	428013	6150332
60	428072	6149774
61	428132	6149216
62	428191	6148659
63	428250	6148101
64	428310	6147543
65	428454	6151447
66	428513	6150889
67	428573	6150332
68	428632	6149774
69	428692	6149216
70	428751	6148659
71	428811	6148101
72	428870	6147543
73	429014	6151447
74	429074	6150889
75	429133	6150332
76	429193	6149774
77	429252	6149216
78	429312	6148659
79	429371	6148101
80	429431	6147543

Bibliography

[1] M. Zaaijer, "Great expectations for offshore wind turbines: Emulation of wind farm design to anticipate their value for customers," PhD thesis, TU Delft, Delft University of Technology, 2013.

[2] G. Katsouris, "Infield cable topology optimization of offshore wind farms," 2015.

[3] W. Program, "Wind turbine power ouput variation with steady wind speed." [Online]. Available: http://www.wind-power-program.com/turbine_characteristics.htm

[4] S. S. Perez-Moreno, "Model fidelity selection for multi-disciplinary design analysis and optimisation of offshore wind farms," November 2015.

[5] G. van Rossum, "Python programming language," 1989. [Online]. Available: https://www.python.org/

[6] J. F. M. Christopher N. Elkinton and J. G. McGowan, "Offshore wind farm layout optimization (owflo) project: Preliminary results," *University of Massachusetts, Amherst, MA 01003*, January 2006.

[7] C. M. Bruun and C. B. Hasager, "Wake effects of large offshore wind farms identified from satellite sar," *Remote Sensing of Environment*, vol. 98, no. 2, pp. 251–268, 2005.

[8] J. F. Ainslie, "Calculating the flowfield in the wake of wind turbines," *Journal of Wind Engineering and Industrial Aerodynamics*, vol. 27, no. 1, pp. 213–224, 1988.

[9] F. B. Guillén, "Development of a design tool for offshore wind farm layout optimization," *Technische Universiteit Delft, Eindhoven, The Netherlands, Master of Science Thesis*, 2010.

[10] L. Martin, "Wind energy–the facts: A guide to the technology, economics and future of wind power," 2010.

[11] D. V. Hertem, O. Gomis-Bellmunt, and J. Liang, *HVDC Grids for Transmission of Electrical Energy: Offshore Grids and a Future Supergrid*, 2016.

[12] J. Bauer and J. Lysgaard, "The offshore wind farm array cable layout problem: a planar open vehicle routing problem," *Journal of the Operational Research Society*, vol. 66, no. 3, pp. 360–368, 2014.

[13] A. Amberg, W. Domschke, and S. Voß, "Capacitated minimum spanning trees: Algorithms using intelligent search," 1996.

[14] ABB, XPLE, "Submarine cable systems: Attachment to xlpe land cable systems-users guide," 2010.

[15] S. Lundberg, "Performance comparison of wind park configurations," *Chalmers University of Technology*, 2003.

[16] P. Nielsen, "Offshore wind energy projects, feasibility study guidelines," *SEAWIND Altener project-Feasibility Study Guidelines (EMD)*, 2003.

[17] M. Dicorato, G. Forte, M. Pisani, and M. Trovato, "Guidelines for assessment of investment cost for offshore wind generation," *Renewable Energy*, vol. 36, no. 8, pp. 2043–2051, 2011.

[18] 4C Offshore, "Support structures fo roffshore wind turbines," June 2013. [Online]. Available: http://www.4coffshore.com/windfarms/support-structures-for-offshore-wind-turbines-aid3.html

[19] Wind Energy, THE FACTS, "Offshore support structures." [Online]. Available: http://www.wind-energy-the-facts.org/offshore-support-structures.html

[20] LORC, "Horns rev 1 offshore wind farm." [Online]. Available: http://www.lorc.dk/offshore-wind-farms-map/horns-rev-1

[21] G. van Bussel, "Offshore wind farm aspects," *Offshore Wind Farm Design*.

[22] P.-E. Rethore, P. Fuglsang, T. J. Larsen, T. Buhl, and G. C. Larsen, "Topfarm wind farm optimization tool," *Risó DTU, National Laboratory*, February 2011.

Glossary

List of Acronyms

OWF	Offshore Wind Farms
LCOE	Levelized Cost of Electricity
RES	Renewable Energy Sources
OWFICTP	Offshore Wind Farm Infield Cable Topology Problem
CMST	Capacitated Minimum Spanning Tree
EW	Esau-Williams
GA	Genetic Algorithm
POS	Planar Open Savings
LPC	Levelized Production Cost
ICT	Infield Cable Topology
OWT	Offshore Wind Turbines